

## Review Article

## Effects of Iron Oxide Nanoparticles: Cytotoxicity, Genotoxicity, Developmental Toxicity, and Neurotoxicity

Vanessa Valdiglesias,<sup>1</sup> Gözde Kiliç,<sup>1,2</sup> Carla Costa,<sup>3,4</sup>  
 Natalia Fernández-Bertólez,<sup>1,2</sup> Eduardo Pásaro,<sup>1,2</sup>  
 João Paulo Teixeira,<sup>3,4\*</sup> and Blanca Laffon<sup>1</sup>

<sup>1</sup>DICOMOSA Group, Department of Psychology, Area of Psychobiology, Universidade da Coruña, Spain

<sup>2</sup>Department of Cell and Molecular Biology, Universidade da Coruña, Spain

<sup>3</sup>Department of Environmental Health, Portuguese National Institute of Health, Porto, Portugal

<sup>4</sup>EPI Unit—Institute of Public Health, University of Porto, Portugal

Iron oxide nanoparticles (ION) with superparamagnetic properties hold great promise for use in various biomedical applications; specific examples include use as contrast agents for magnetic resonance imaging, in targeted drug delivery, and for induced hyperthermia cancer treatments. Increasing potential applications raise concerns over their potential effects on human health. Nevertheless, very little is currently known about the toxicity associated with exposure to these nanoparticles at different levels of biological organization. This article provides an overview of recent studies evaluating ION cytotoxicity, genotoxicity, developmental toxicity and neurotoxicity. Although the results of these studies are sometimes controversial,

they generally indicate that surface coatings and particle size seem to be crucial for the observed ION-induced effects, as they are critical determinants of cellular responses and intensity of effects, and influence potential mechanisms of toxicity. The studies also suggest that some ION are safe for certain biomedical applications, while other uses need to be considered more carefully. Overall, the available studies provide insufficient evidence to fully assess the potential risks for human health related to ION exposure. Additional research in this area is required including studies on potential long-term effects. *Environ. Mol. Mutagen.* 00:000–000, 2014. © 2014 Wiley Periodicals, Inc.

**Key words:** iron oxide nanoparticles; cytotoxicity; genotoxicity; developmental toxicity; neurotoxicity

### INTRODUCTION

An engineered nanomaterial may be defined as any intentionally produced material that has a characteristic size from 1 to 100 nm in at least one dimension. Because of this very small size and the resultant high surface to volume ratio, nanomaterials exhibit properties that are different from larger-sized materials of the same chemical composition [Landsiedel et al., 2012]. Nanotechnology (technology using nanomaterials) has taken advantage of most of these new properties and so has expanded into various domains from industrial applications (e.g., which may lead to stronger and lighter building materials) and biomedical uses (e.g., as new tools for the diagnosis and treatment of diseases) to commercially available consumer products including transparent sunscreens, stain-resistant clothing, self-cleaning glass, paints, sports equip-

ment, etc. [Rosi et al., 2005; Card et al., 2008; Iavicoli et al., 2012].

Grant sponsor: Xunta de Galicia; Grant number: EM 2012/079; Grant sponsor: MODENA COST Action; Grant number: TD1204; Grant sponsor: University of A Coruña (to G.K.).

Vanessa Valdiglesias and Gözde Kiliç contributed equally to this work. João Paulo Teixeira and Blanca Laffon contributed equally to the senior authorship of this manuscript.

\*Correspondence to: João Paulo Teixeira, Department of Environmental Health, Portuguese National Institute of Health, Rua Alexandre Herculano, 321, Porto 4000-055, Portugal. E-mail: jpft12@gmail.com

Received 2 April 2014; provisionally accepted 6 August 2014; and in final form 22 August 2014

DOI 10.1002/em.21909

Published online 00 Month 2014 in Wiley Online Library (wileyonlinelibrary.com).

The development of nanotechnology has resulted in a growing public debate on the toxicity and environmental impact of nanomaterials. The reduction in size provides greater bioavailability as compared to the bulk material, leading to enhanced absorption of nanoparticles in biological systems [Das et al., 2009]. Living organisms are made of cells that usually range 10 to 100  $\mu\text{m}$ . However, cellular parts are much smaller, and proteins are even smaller with a typical range of just 5 to 50 nm. These size differences enable the potential use of nanoparticles as very small probes to directly observe cellular machinery without too much interference [Taton, 2002; Salata, 2004]; however, nanomaterials can also interact with cellular components and induce toxic effects. Indeed, particle toxicology suggests that, for toxic particles in general, more particle surface equals more toxicity [Borm et al., 2006].

Although numerous studies have demonstrated different toxic effects associated with exposure to nanomaterials, including mitochondrial damage, oxidative stress, chromosomal and oxidative DNA damage, altered cell cycle regulation and protein denaturation [Gurr et al., 2005; Nel et al., 2006; Carlson et al., 2008; Karlsson et al., 2008; Pan et al., 2009; Ahamed et al., 2012], very little is still known about the underlying mechanisms responsible for the toxic actions of nanoparticles. One of the most frequently suggested mechanisms involved in toxicity is the generation of reactive oxygen species (ROS) and development of oxidative stress, thereby triggering an inflammatory response by modulating intracellular calcium concentrations, activating transcription factors and inducing cytokine production [Buzea et al., 2007; Oberdorster et al., 2008; Moller et al., 2010]. Inflammation and oxidative stress are responsible for damaging biomolecules—including lipids, proteins and DNA—thus promoting cell and tissue damage that can culminate in genotoxic, cytotoxic and fibrotic responses that are associated with disease [Johnston et al., 2013]. Nevertheless, one of the main reasons for the lack of information on the mechanisms of action of nanomaterials is that simple and standardized screening methods for nanoparticle toxicity have yet to be established [Auffan et al., 2009; Guichard et al., 2012].

Magnetic nanoparticles, made of iron, cobalt, or nickel oxides, are nanomaterials of great interest, particularly in biomedicine fields. Due to their magnetic properties they can be manipulated by an external magnetic field gradient. Thus, as a result of the intrinsic penetrability of magnetic fields into human tissue, they can be directed to a targeted region of the body to deliver a package, such as a drug or a gene [Pankhurst et al., 2003], or to be used as colloidal mediators for induced hyperthermia cancer treatments [Jordan et al., 1999]. They also have applications as contrast agents for magnetic resonance imaging (MRI) [Lee et al., 2007]. Furthermore, nanoparticles that are

made of a ferro- or ferromagnetic material can exhibit a unique form of magnetism called superparamagnetism, which is highly useful in most biomedical applications [Huber, 2005]. Each magnetic particle becomes a single magnetic domain and shows superparamagnetic behavior when its size is below a critical value, which is dependent on the material (but is typically around 10–20 nm) and when the temperature is above the so-called blocking temperature [Lu et al., 2007]. This means that each individual particle has a large constant magnetic moment and behaves like a giant paramagnetic atom with a fast response to applied magnetic fields, and with negligible remanence (residual magnetism) and coercivity (the field required to bring the magnetization to zero). In contrast to multiple-domain ferromagnetic materials that retain their magnetism even after the removal of the magnetic field, superparamagnetic nanoparticles lose their magnetization when the magnetic field is switched off. This feature makes superparamagnetic nanoparticles very attractive for a broad range of biomedical applications because they maintain their colloidal stability, and so the risk of forming agglomerates is negligible at room temperature. The maximum volume particle that can be superparamagnetic at a given temperature varies directly with the magnetocrystalline anisotropy. This means that iron nanoparticles are superparamagnetic at much larger size than particles of any other magnetic metal [Huber, 2005].

There are several types of iron oxide nanoparticles (ION), such as hematite ( $\alpha\text{-Fe}_2\text{O}_3$ ), maghemite ( $\gamma\text{-Fe}_2\text{O}_3$ ) and magnetite ( $\text{Fe}_3\text{O}_4$ ), among which the latter is very promising because of its proven biocompatibility [Gupta and Gupta, 2005]. The term ION includes both superparamagnetic iron oxide nanoparticles (SPION) and magnetic ION; these terms are interchangeably used in the literature. For such biomedical applications, these nanoparticles must have multifunctional characteristics, including optimized size and modified surface [Hong et al., 2011]. ION can be metabolized and easily release iron ions, which can be transported by proteins like ferritin, transferritin and hemosiderin, and they can be stored in endogenous iron reserves of the body for later use [Santhosh and Ulrih, 2013]. That fact that it is well known that iron ions, and several other transition metal ions, have the ability to generate ROS and stimulate the peroxidation of cell membrane lipids [Stohs and Bagchi, 1995; Singh et al., 2012], reinforces the necessity for risk assessment and safety regulations of iron oxide nanoparticles.

The use of ION in biomedical research is progressively gaining importance, leading to the rapid development of novel ION types. Figure 1 summarizes the scientific reports on ION published since 1989, showing a dramatic increase in publications since the early 21st century. Therefore, as a consequence, a growing number of toxicological studies have now been carried out with a great

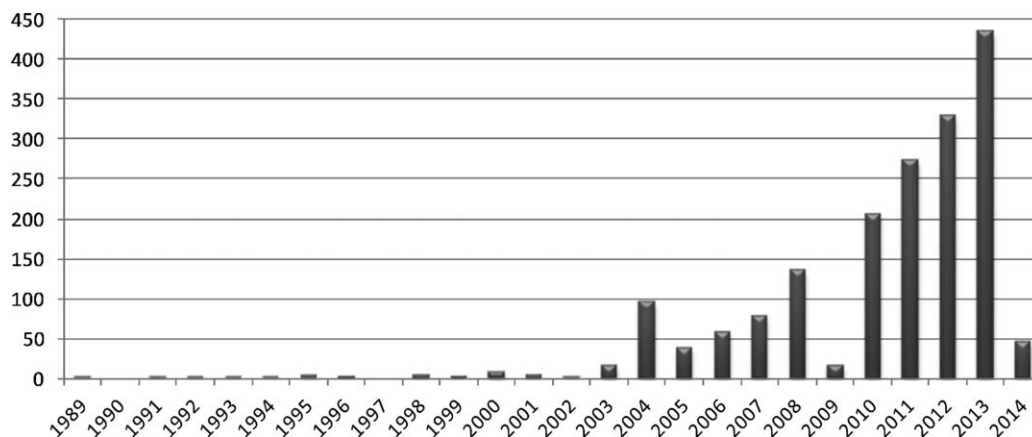


**Fig. 1.** Number of scientific studies published on ION (Source: PubMed). Search terms: "iron oxide nanoparticles." Date of search: February 2014.

variety of ION, cell types, incubation conditions, etc. However, it is still unclear whether ION is generally safe or should be used prudently. In order to improve knowledge in this field, the aim of this work was to compile and review the data available on adverse effects related to exposure to ION, including cytotoxicity, genotoxicity, neurotoxicity and developmental toxicity, in addition to considering the different ION types and surface modifications. Review of these studies helps to fill the significant knowledge gap on the ION toxicological profile and highlights the most imperative research needs in this field.

### SURFACE MODIFICATION OF IRON OXIDE NANOPARTICLES

A common problem associated with nanoparticles is their intrinsic instability over long periods of time, since they tend to form agglomerates to reduce the energy associated with the high surface area to volume ratio. Moreover, naked nanoparticles can be easily trapped by the immune system as foreign materials, which means that they cannot reach the target [Santhosh and Ulrich, 2013]. Furthermore, naked metallic nanoparticles are highly chemically active, and are easily oxidized in air, generally resulting in loss of magnetism and dispensability [Lu et al., 2007]. In order to minimize these effects, the surface of commercially available nanoparticles may be modified by coating with different materials including: polymeric coatings, natural (gelatine, dextran, chitosan, pullulan, etc.) or synthetic (polyethylene glycol [PEG], polyacrylic acid, polyvinyl alcohol, etc.), inorganic molecules (silica, gold, silver, platinum, palladium, iron, carbon) and numerous biological molecules (polypeptides, proteins, antibodies, biotin, etc.). Surface modification often serves multiple purposes [Kim et al., 2012]. On one hand, it stabilizes nanoparticles in an environment of

slightly alkaline pH or high salt concentrations. For example, ION coated with silica, which achieves the isoelectric point at pH of 2 to 3, are negatively charged at blood pH, helping to avoid aggregate formation in body fluids [McBain et al., 2008]. On the other hand, surface modification allows biomolecule binding favoring surface attachments between ION and antibodies, peptides, hormones or drugs [Sadeghiani et al., 2005]. The polymer coating significantly increases their overall size, which may also be used to modify the biodistribution of the particles, since it may limit their tissue distribution, penetration, and metabolic clearance [Wang et al., 2001; Bjørnerud and Johansson, 2004]. Moreover, the use of surface coatings by forming monolayers on the nanoparticle surface, such as stable gold or silica shell structures, allows for the application of core materials that would be toxic otherwise.

Certain nanomaterials are attractive probe candidates in biodiagnostic assays, not only because of their large surface-to-volume ratio, their chemically modifiable physical properties and their overall structural robustness, but also due to their unusual target binding properties [Rosi and Mirkin, 2005]. The potential of the surface coatings that enable special probing and/or monitoring of local physical mechanistic changes at a length scale would greatly assist in improving disease detection, monitoring, and treatment [Sun et al., 2008]. For this purpose ION are required to be magnetically targeted to a particular tissue/organ in order to benefit a therapeutic or diagnostic application. Moreover, in a study using a number of cell lines it was demonstrated that cellular uptake efficiency of ION is dependent on surface coating of the nanoparticles, irrespective of the cell line used [Zhu et al., 2012b]. Hence, a strategy to adjust the cellular uptake efficiency and precision of ION is to modify their surface coating.

Some commonly used coatings for ION are: (a) PEG—which is an ideal coating material because of its good

compatibility, favorable chemical properties, and solubility [Yu et al., 2012], (b) silica—widely used for bioimaging and bio-sensing purposes as its transparent matrix allows the efficient passage of excitation and emission light through them [Alwi et al., 2012], (c) carboxydextran—which provides stability and increases intravascular retention time of nanoparticles and is used for cell labeling [Tong et al., 2011], (d) polyethylene imine—with high cellular uptake, so it is used as gene/drug delivery vehicle [Xia et al., 2009], and (e) other polymeric and non-polymeric coatings are also used [reviewed in Gupta and Gupta, 2005; Santhosh and Ulrih, 2013].

Together with providing a general increased biocompatibility, the surface coating may also alter the ION toxicity [reviewed in Singh et al., 2010]. For example, a study investigating the effects of different surface coatings on cell behavior and morphology reported that dextran-coated magnetite nanoparticles induced more prominent membrane disruptions than uncoated nanoparticles, although cell death and reduced cell proliferation was similar for both of them; however, albumin-coated magnetite did not show cytotoxic effects [Berry et al., 2003]. Similarly, an *in vitro* study on A3 human T lymphocytes showed that ION coated with carboxyl groups have a higher cytotoxicity (fluorescein diacetate assay and WST-1 assay) than those coated with amine groups [Ying and Hwang, 2010]. Therefore, it is important to carefully monitor the influence of the surface modifications (coating, functional groups, and net size) on ION toxicity.

## TOXIC EFFECTS OF IRON OXIDE NANOPARTICLES

ION have attracted much attention not only because of their superparamagnetic properties, which make them suitable for interesting biomedical applications, but also because they are associated with low toxicity in the human body [Hussain et al., 2005; Jeng and Swanson, 2006; Karlsson et al., 2009]. Thus, in general, ION are classified as biocompatible [Kunzmann et al., 2011]. For example, an *in vitro* study comparing several metal oxide nanoparticles showed ION to be non-cytotoxic below 100  $\mu\text{g/ml}$  [Karlsson et al., 2008]. However, the absence of cytotoxicity does not guarantee that ION pose no risk for use in specific applications, as recent studies report different harmful cellular effects including DNA damage, oxidative stress, mitochondrial membrane dysfunction, and changes in gene expression as a result of ION exposure in the absence of cytotoxicity [reviewed in Singh et al., 2010]. Hence, criteria to define the toxicity of nanoparticles must be clearly defined [Huang et al., 2012], and it has been suggested that terms such as “biocompatibility” be re-evaluated [Singh et al., 2010]. Nevertheless, in a review on application of magnetic nanoparticles for drug delivery, Kim et al. [2012] sug-

gested that the possible toxicity of these nanoparticles does not mean that they cannot be applied biomedically, but optimal benefits and potential risks need to be identified.

Among the different mechanisms that are potentially involved in nanoparticle toxicity in the body, it seems that most toxicity from magnetic ION arise from the production of excess ROS [Nel et al., 2006; Unfried et al., 2007; Shubayev et al., 2009; Soenen and De Cuyper, 2009]. High ROS levels can damage cells by producing lipid peroxidation, mitochondrial damage, DNA disruption, gene transcription modulation, and protein oxidation, which can then trigger a cascade of  $\text{Ca}^{+2}$ -dependent signaling mechanisms resulting in a decline in physiological functions and cell apoptosis/death [Stroh et al., 2004]. However, other toxic effects in addition to ROS production, including cell cycle alterations and induction of apoptosis, occur in different cell types after ION treatment [Soenen et al., 2011; Wu et al., 2013].

Despite these studies, information regarding the possible risk of ION exposure to humans is still very limited and conflicting. Work addressing the potential toxic effects of ION is mainly focused on evaluating cytotoxic effects—principally changes in viability, cytoskeleton disruptions or ROS production—in *in vitro* cell cultures. Much less is known about their toxicity to genetic material, the nervous system, or embryonic development, and other endpoints. In the following sections, together with going over the main results on ION cytotoxicity, current knowledge on the ION effects at different levels of biological organization are reviewed and the main gaps of information are indicated.

### Cytotoxicity

Figure 2 shows the number of articles published to date on ION cytotoxicity, classified by the endpoint evaluated. The most frequent outcome reported is oxidative damage, followed by analysis using the MTT (3-[4,5-dimethylthiazol-2-yl]-2,5 diphenyl tetrazolium bromide) assay (viability based on mitochondrial functionality), other measures of viability different using the MTT and LDH (lactate dehydrogenase) assays, and assessment cell cycle effects. As an extensive review of ION cytotoxicity was included in several previous papers [Soenen and De Cuyper, 2009; Suh et al., 2009], in this review we focus on the most recent studies summarizing the main cytotoxic effects evaluated after ION exposure.

Magnetite/maghemite combinations have already been approved for clinical use as MRI contrast agents [Gould, 2006]. Nevertheless, there are some inconsistencies in the literature about the cytotoxicological assessment in different cells and the interpretation of these results. Based on this review, it appears that dose, exposure time and cell type are factors affecting the results obtained. For

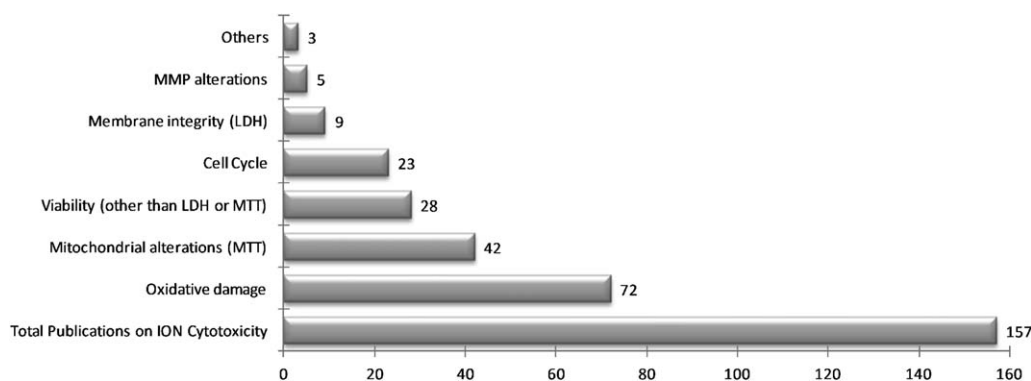


**Fig. 2.** Literature review on ION studies evaluating different cytotoxicity outcomes (MMP: mitochondrial membrane potential; LDH: lactate dehydrogenase assay; MTT: 3-(4,5-dimethylthiazol-2-yl)-2,5-diphenyltetrazolium bromide) assay. Source: PubMed. Date of search: February 2014.

example, Iron (II,III) oxide nanoparticles induced moderate time- and concentration-dependent cytotoxicity in Vero cells after 24 hr exposure (MTT assay); however, they proved to be devoid of mutagenic effect (bacterial reverse mutation assay in *Salmonella typhimurium* and *Escherichia coli*), and they did not induce histopathological changes in rats after a single intratracheal instillation [Szalay et al., 2012]. A slight degree of cytotoxicity, evaluated by trypan blue exclusion, in human alveolar epithelial A549 cells was also reported for Fe<sub>2</sub>O<sub>3</sub> nanoparticles, but not for Fe<sub>3</sub>O<sub>4</sub> nanoparticles [Karlsson et al., 2009]. In addition, biocompatibility tests on L-929 fibroblast cells using the MTT assay revealed very little generation of cytotoxicity for either Fe<sub>3</sub>O<sub>4</sub> at mesoporous silica composites (potentially used for drug delivery) [Huang et al., 2012] or various ION coated with polyvinyl alcohol (PVA) [Mahmoudi et al., 2009]. Although in another study using L-929 fibroblasts ION modified with different functional groups induced a dose-dependent reduction in viability, using highly water-soluble tetrazolium salt (WST-8, similar to MTT), the observations suggested that ION concentration is more critical for cytotoxicity than any other factor including surface modification or size [Hong et al., 2011]. Nevertheless, ION cytotoxicity was also reported to be mainly dependent on nanoparticle size and surface coating [Ying and Hwang, 2010; Rivet et al., 2012]. Thus, uncoated Fe<sub>3</sub>O<sub>4</sub> nanoparticles were not cytotoxic (trypan blue exclusion assay), while oleate-coated Fe<sub>3</sub>O<sub>4</sub> nanoparticles were cytotoxic in a dose-dependent manner, and intrinsic properties of sodium oleate were excluded as a cause of the toxic effect [Magdolenova et al., 2013]. Furthermore, a comparative cytotoxicity study (measuring intracellular enzymatic activity with calcein-AM and membrane disruption with ethidium homodimer-1) in a human cervical cancer cell line (HeLa) and an immortalized normal human retinal pigment epithelial cell line (RPE) indicated that, although uncoated magnetite nanoparticles at a high concentration

(0.40 mg/ml) were toxic to both HeLa and RPE cells, their cytotoxicity at low concentrations was cell-type specific, with RPE cells being more susceptible than HeLa cells [Li et al., 2012].

Investigations aimed at using ION-labeled stem cells in regenerative therapies did not report cytotoxic effects for these nanoparticles. No effects on cardiac differentiation potential and functional properties of mouse embryonic stem cells were observed over a time course of 1 to 2 weeks of in vivo non-invasive tracking of ION-labeled transplanted cells [Au et al., 2009]. In addition, no significant toxicity and successful chondrogenesis occurred in human mesenchymal stem cells incubated for 24 or 72 hr with ferucarbotran (a clinically approved and commercially available carboxydextran-coated ION that is used as a negative MRI contrast agent for hepatic imaging) [Yang et al., 2011]. Likewise, carboxydextran-coated ION internalization did not alter survival, cell cycle, proliferation, metabolism, and phenotype of human Amniotic Fluid Cells (hAFC), and the transplantation of ION-labeled hAFC in the lateral ventricles of wobbler (a murine model of amyotrophic lateral sclerosis) did not influence mouse survival [Bigini et al., 2012]. On the basis of these studies, ION seem to be safe for tracking the fate of transplanted stem cells. However, several reports have stated that these particles can in fact exert large effects on cell wellbeing [reviewed in Soenen and De Cuyper, 2009].

Numerous studies showing cytotoxicity following ION exposure relate this effect to oxidative stress and ROS generation [Auffan et al., 2008; Buyukhatipoglu and Clyne, 2011; Ahamed et al., 2012; Zhang et al., 2012; Dwivedi et al., 2014; Malvindi et al., 2014]. ROS production, glutathione depletion and inactivation of several antioxidant enzymes were observed in Chinese hamster lung cells after 36 hr of exposure to L-glutamic acid-coated ION (Fe<sub>2</sub>O<sub>3</sub>) [Zhang et al., 2012]. Also, when ION coated with Tween 80 were applied at 300 µg/ml

and higher concentrations for 6 hr, the viability of murine macrophage J774 cells decreased significantly; these effects were not detected at lower concentrations or earlier exposure times and were related to enhanced intracellular ROS generation [Naqvi et al., 2010]. However, although 24 hr exposure of A549 cells to magnetite in the nano-range enhanced ROS production and increased mitochondrial membrane depolarization to a significant extent, and the nanoparticles were effectively internalized by endocytosis, this effect was not accompanied by cytotoxicity [Könczöl et al., 2011]. In contrast, Pd-coated magnetite nanoparticles did not initiate ROS production and caused little impact on the viability of human skin (HaCaT) and colon (CaCo-2) cell lines, and on a rainbow trout gill cell line (RTgill-W1), even at very high concentrations [Hildebrand et al., 2010]; thus, the authors suggested that modification of the surface coating could mediate the cytotoxicity of ION.

ROS were also reported to be induced by ION in different studies in vascular endothelial cells. ION (maghemite) were efficiently taken up by human umbilical vascular endothelial cells (HUVEC), but provoked cell death 24 hr after the exposure, most likely through the oxidative stress pathway [Hanini et al., 2011]. Similarly, Fe<sub>2</sub>O<sub>3</sub> and Fe<sub>3</sub>O<sub>4</sub> nanoparticles were proposed to affect the endothelial system by generating oxidative stress and inducing cytotoxicity and suppression of cellular viability in human aortic endothelial cells [Zhu et al., 2011]. Induced ROS production by ION (maghemite) in human microvascular endothelial cells was also reported to enhance cell permeability through the remodeling of microtubules [Apopa et al., 2009]. Likewise, dose- and time-dependent intracellular ROS formation (which increased more than 800% after 3 hr of exposure at 0.5 mg/ml) and decrease in cell viability was reported in porcine aortic endothelial cells treated with bare ION; in addition, previous incubation with the ROS scavengers *N*-acetyl cysteine and sodium pyruvate enhanced cell viability [Buyukhatipoglu and Clyne, 2011].

Upon metabolization of ION, free iron can be shuttled out of the endocytic compartment into the normal cellular iron pool [Soenen and De Cuyper, 2010]. Iron is an innate metal that is essential for life, mainly because of its ability to accept and donate electrons readily by switching between ferrous (Fe<sup>2+</sup>) and ferric (Fe<sup>3+</sup>) ions [Kim et al., 2012]. This reduction-oxidation reaction plays a critical role in energy production and in many other metabolic pathways such as DNA synthesis, mitochondrial oxidative phosphorylation, oxygen transport, and cytochrome P450 function [Shander et al., 2009]. The total quantity of iron in the body is tightly regulated, because excess iron can be extremely toxic; therefore, it is important to avoid administration of ION in high doses or repeated dosing over a short time interval in order not to exceed the normal capacity for handling of iron [Kunz-

mann et al., 2011]. This metal can affect cellular functionality (e.g., by altering the level of transferrin receptor expression) [Schäfer et al., 2007], as well as cellular proliferation capacity [Huang et al., 2009], among others. Moreover, organs such as heart, liver, and pancreatic beta cells, which have highly active mitochondria, are especially vulnerable to iron toxicity [Eaton and Qian, 2002]. Recently, Malvindi et al. [2014] demonstrated that ION coated with silica were able to release iron ions when they were suspended in an acidic medium (pH 4.5), mimicking the lysosomal environment, but not under neutral conditions employing ultrapure water or cell culture medium (pH 7), suggesting that these ION must be internalized by cells before releasing ions. Indeed, increased intracellular iron levels were found in different cells after ION exposure, though usually not initially associated with cytotoxicity [Geppert et al., 2009, 2011; Rosenberg et al., 2012]. However, the degradation rate of ION, and consequently their ability to release iron ions, is influenced by the presence/absence of coating and the physical-chemical properties of the coating [Levy et al., 2010; Mahon et al., 2012].

Together with ROS production and iron ion release, other forms of cytotoxicity reported after ION exposure that may be or may be not related to these mechanisms include cell cycle alterations [Wu and Sun, 2011], decreases in cell viability [Wang et al., 2010a], cytoskeleton alterations [Wu et al., 2010], and disruption of mitochondrial membrane potential [Zhu et al., 2010].

### Genotoxicity

Most studies on the genetic toxicity of nanomaterials in the literature use standard genotoxicity tests (Table I). In vitro DNA damage tests (especially the comet assay) and in vitro chromosome mutation assays (especially micronucleus [MN] test) are the most frequently employed to evaluate ION genotoxicity. In general, the results of these published ION genotoxicity studies are inconsistent, even at similar doses. A positive response was observed in A549 alveolar cells treated with bare nanomagnetite both in the comet assay and MN test, but the damaging effect was reduced by simultaneous exposure to *N*-acetylcysteine or by pretreatment with butylated hydroxyanisole, both ROS scavengers [Könczöl et al., 2011]. However, it was recently reported that oxidative stress plays, at most, a marginal role in the induction of genotoxicity (evaluated by comet assay) by surface-modified magnetite nanoparticles [Mesárošová et al., 2014]. MN induction was also observed in human MCL5 lymphoblastoid cells treated with dextran-coated  $\gamma$ -Fe<sub>2</sub>O<sub>3</sub> nanoparticles for 24 hr [Singh et al., 2012]. In addition, comet assay evaluation of murine L-929 fibroblast cells treated with ION coated with (3-aminopropyl)trimethoxysilane (APTMS), tetraethyl orthosilicate (TEOS)-APTMS, or citrate showed

TABLE I. Studies on Genotoxicity of ION (Ordered Chronologically)

Reference	ION type and surface modification	Physical-chemical characterization	Cellular model/organism	Methods	Treatment conditions	Results
Weissleder et al. [1989]	AMI-25 ION	Volume median diameter of particles (LLS): 80nm	<i>S. typhimurium</i> (strains TA-1535, TA-1537, TA-1538, TA-90 and TA-100)	Ames test	0.008 to 12 mg Fe/plate with and without metabolic activation	The test did not reveal an increased number of histidine revertant colonies after incubation with or without metabolic activation
Freitas et al. [2002]	Magnetite coated with dodecanoic acid and ethoxylated alcohol	Diameter 9.4 nm	Female Swiss mouse bone marrow cells	MN test	Intraperitoneally treated with magnetic fluid containing $5 \times 10^{15}$ , $5 \times 10^{16}$ , and $5 \times 10^{17}$ particles/kg; MN assay—24 hr after application	ION induced MN formation at all concentrations tested.
Sadeghiani et al. [2005]	Magnetite coated with polyaspartic acid (PAMF)	Average core particle diameter (TEM): 8.5 nm	Female Swiss mouse bone marrow cells	MN test	Intravenously treated with 50 ml of the PAMF containing $0.6 \times 10^{16}$ or $1.6 \times 10^{16}$ particle/ml. MN test—1, 7, 15, and 30 days after application	ION induced MN formation at both concentrations tested
Auffan et al. [2006]	DMSA-coated Fe <sub>2</sub> O <sub>3</sub>	Shape roughly spherical. Diameter size 6 nm. SSA (BET): 172 m <sup>2</sup> /g. Colloidal stability in media: no destabilization for concentration lower than 10 <sup>-3</sup> g/l.	Human dermal fibroblasts	Comet assay	$10^{-6}$ to $10^{-1}$ g/l for 2 and 24 hr	No genotoxic effects were observed
Bourrinet et al. [2006]	Dextran-covered magnetite (Ferumoxtran-10)	Mean diameter (TEM): 4.3–4.9 nm	<i>S. typhimurium</i> (strains TA1535, TA1537, TA98, TA100, and TA102)	Ames test	Five concentrations from 315 to 5047 µg Fe/plate, with or without metabolic activation system, for 48 to 72h	Ferumoxtran-10 did not induce any significant increase in the number of revertants
			Chinese hamster ovary cells	CA	400 to 4000 µg Fe/ml, with or without metabolic activation for 2 to 7 hr	No significant increase of CA was observed at any concentration tested, with or without metabolic activation.
			Mice	MN test	Intravenous administration of 250, 500 and 1000 mg Fe/Kg. Mice were killed 24, 48 and 72 hr after dosing	No clastogenic activity was seen after treatments
			Rat hepatocytes	DNA repair assay	4, 40 and 400 mg Fe/Kg for 2 and 16 hr	The results produce a range of values with less than 2% of cells in DNA repair.

TABLE I. (continued).

Reference	ION type and surface modification	Physical-chemical characterization	Cellular model/organism	Methods	Treatment conditions	Results
Karlsson et al. [2008]	CuZnFe <sub>2</sub> O <sub>4</sub>	Particle size (TEM): 10–100 nm. DLS size: 40–300 nm and zeta potential: 34.2 mV. Surface area in powder 18 m <sup>2</sup> /g	Human lung adenocarcinoma A549 cells	Comet assay (with and without FPG enzyme)	1, 20, 40 mg/ml for 4 hr	Positive results for both experiments
Bhattacharya et al. [2009]	Fe <sub>2</sub> O <sub>3</sub>	Surface area (BET): 34.39 ± 0.17 m <sup>2</sup> /g. Zeta potential and particle size distribution by DLS: -28.68 mV; ~50 nm. EDX spectral analysis of surface chemistry: purely composed of 78.7% Fe and 21.3% O <sub>2</sub> . Morphology (SEM): spherical shape	Human lung diploid IMR-90 fibroblasts and human bronchial epithelial BEAS-2B cells (SV-4 virus transformed)	Comet assay	2, 5, 10, 50 mg/cm <sup>2</sup> , for 24 hr	Positive at 10 and 50 mg/cm <sup>2</sup> in IMR-90, and at 50 mg/cm <sup>2</sup> in BEAS-2B
Karlsson et al. [2009]	Fe <sub>3</sub> O <sub>4</sub> and Fe <sub>2</sub> O <sub>3</sub>	Fe <sub>3</sub> O <sub>4</sub> : Particle size (TEM): 20–40 nm; DLS size: <200 nm and zeta potential: 1.8 mV; SSA (BET): 42 m <sup>2</sup> /g. Fe <sub>2</sub> O <sub>3</sub> : Particle size (TEM): 30–60 nm; DLS size: 1580 nm and zeta potential: -17.3 mV; SSA in powder 40 m <sup>2</sup> /g	Human lung adenocarcinoma A549 cells	Comet assay (with and without FPG enzyme)	1, 20, 40 mg/ml for 4 hr	ION did not induce 8-OHdG-adduct formation
Wu et al. [2010]	Fe <sub>3</sub> O <sub>4</sub> loaded with daunorubicin	n/a	Kunming mouse bone marrow cells	MN test	1.25, 2.50, 3.75, and 5.00 g/kg of ION intraperitoneally injected twice with a 24 hr interval	Negative results for both experiments for Fe <sub>2</sub> O <sub>3</sub> . For Fe <sub>3</sub> O <sub>4</sub> , negative results for standard comet assay but positive for oxidative DNA damage
Estevanato et al. [2011]	Maghemite (γ-Fe <sub>2</sub> O <sub>3</sub> ) encapsulated within albumin based nanospheres (MAN)	Average diameter (TEM): MAN: 73.0 ± 3.0 nm; maghemite: 8.9 ± 0.1 nm.	Female Swiss mouse bone marrow erythrocytes	MN test	Mice were intraperitoneally treated with 100 ml of MAN suspension for 1, 2, 7, 15 and 30 days	No MN induction was observed in any case
Hong et al. [2011]	Fe <sub>3</sub> O <sub>4</sub> bare and modified with various functional groups (-OH, -COOH, -NH <sub>2</sub> ) by coating with TEOS, APTMS, TEOS-APTMS, and citrate	Average particle sizes and shapes (TEM): Bare, APTMS and citrate coated: 1 nm; TEOS and TEOS-APTMS coated: 15 nm. Zeta potential (mV): Bare: -20 mV; TEOS: -30 mV; APTMS: 25 mV; TEOS-APTMS: 30 mV; citrate: -40 mV	Murine L-92 fibroblasts from subcutaneous connective tissue	Comet assay	100, 200, 1,000 ppm for 24 hr	No damage to DNA was observed after treatment with bare and TEOS coated Fe <sub>3</sub> O <sub>4</sub> . Cells treated with APTMS, TEOS-APTMS and citrate coated Fe <sub>3</sub> O <sub>4</sub> showed a concentration-dependent increase of DNA damage
Könczöl et al. [2011]	Four size magnetite fractions: bulk magnetite, respirable fraction,	Particle size and shape by SEM: 0.2–10 μm (bulk magnetite), 2–3 μm	Human lung adenocarcinoma A549 cells	MN test	1, 10, 50, 100 mg/cm <sup>2</sup> , for 24 hr; ROS	Increases in MN frequency for all four fractions. NAC decreased MN formation

TABLE I. (continued).

Reference	ION type and surface modification	Physical-chemical characterization	Cellular model/organism	Methods	Treatment conditions	Results
Guichard et al. [2012]	alveolar fraction, and magnetite nanoparticles	(respirable fraction), 0.5–1.0 $\mu\text{m}$ (alveolar fraction), 20–60 nm (nanoparticles). Nanoparticles mean diameter: 311 nm; polydispersity index: 0.481	Syrian hamster embryo cells	Comet assay	scavenger: NAC pretreatment 1, 10, 50, 100 mg/cm <sup>2</sup> , for 4 hr; ROS scavengers: NAC and BHA pretreatment	Dose-dependent increases in DNA damage for all four fractions. NAC and BHA decreased level of DNA damage No significant increase in DNA damage was detected from nanosized and micro-sized ION None of the samples tested showed significant induction of MN formation after 24 hr of exposure
Ma et al. [2012]	Fe <sub>2</sub> O <sub>4</sub> and Fe <sub>2</sub> O <sub>3</sub>	Particle size (TEM, nm): 27 $\pm$ 8 (Fe <sub>2</sub> O <sub>4</sub> nano), 156 $\pm$ 82 (Fe <sub>3</sub> O <sub>4</sub> micro), 35 $\pm$ 14 (Fe <sub>2</sub> O <sub>3</sub> nano), 147 $\pm$ 48 (Fe <sub>2</sub> O <sub>3</sub> micro) SSA (BET, m <sup>2</sup> /g): 40 (Fe <sub>3</sub> O <sub>4</sub> nano), 7 (Fe <sub>3</sub> O <sub>4</sub> micro), 39 (Fe <sub>2</sub> O <sub>3</sub> nano), 6 (Fe <sub>2</sub> O <sub>3</sub> micro)	Kunming male mice: cell suspensions of hepatic and renal tissues	Detection of 8-OHdG by ELISA MN test	Intraperitoneal injections of 5, 10, 20, and 40 mg/kg at a fixed time for 1 week	Significant increase of 8-OHdG levels in liver at highest dose group. In kidney DNA damage was seen in the 20 mg/kg dose and was even greater in the highest-dose group Significant increase in the DPC coefficient at 40 mg/kg dose; no other group had significant increases Only OC-Fe <sub>3</sub> O <sub>4</sub> induced DNA damage especially at the highest concentration
Magdolenova et al. [2012]	Uncoated (U-Fe <sub>3</sub> O <sub>4</sub> ), oleate-coated (OC-Fe <sub>3</sub> O <sub>4</sub> ), Fe <sub>3</sub> O <sub>4</sub>	Nominal size: both 83 nm Concentration: 3 and 7% (w/v), respectively	Cos-1 monkey kidney fibroblasts	DNA-protein cross-links (DPC) determination by SDS assay Comet assay	20 and 40 $\mu\text{g}$ added directly to cells just before embedding cells with agarose	Significant increase in the DPC coefficient at 40 mg/kg dose; no other group had significant increases Only OC-Fe <sub>3</sub> O <sub>4</sub> induced DNA damage especially at the highest concentration
Singh et al. [2012]	Uncoated $\gamma$ -Fe <sub>2</sub> O <sub>3</sub> , dextran-coated $\gamma$ -Fe <sub>2</sub> O <sub>3</sub> , uncoated Fe <sub>3</sub> O <sub>4</sub> , dextran-coated Fe <sub>3</sub> O <sub>4</sub>	Size, morphology and crystallinity by TEM: all $\sim$ 1 nm; crystalline core with inverse spinel structure.	Human lymphoblastoid MCL5 cells	MN test and kinetochore staining; pretreatment with NAC	1–100 mg/ml, for 24 hr	Only dextran-coated $\gamma$ -Fe <sub>2</sub> O <sub>3</sub> induced an increase in MN frequency. Kinetochore staining indicated the predominant induction of chromosome fragmentation. NAC reduced MN frequency Increased levels of TG, 8-oxoG, FapyG, FapyA
		Zeta potential (DLS) for all between –13.9 and 3.3 mV. Hydrodynamic diameter (DLS) in the presence of 10% medium $\sim$ 100 nm, higher in water or in 1% medium		Measurements of oxidative base lesions (8-oxoG, TG, 5-OH-5MeHyd, FapyG, FapyA) by GC/MS	2 and 4 $\mu\text{g}/\text{ml}$ dextran-coated $\gamma$ -Fe <sub>2</sub> O <sub>3</sub> , for 24 hr	

TABLE I. (continued).

Reference	ION type and surface modification	Physical-chemical characterization	Cellular model/organism	Methods	Treatment conditions	Results
Zhang et al. [2012]	L-Glutamic acid (Glu) coated Fe <sub>2</sub> O <sub>3</sub>	Size and morphology (TEM): particles quasi-spherical with an average diameter of 15 nm. Crystal structure (X-ray diffraction analysis): inverse cubic spinel structure. Magnetic measurements (VSM): superparamagnetic behavior	Chinese hamster lung cells	Comet assay and MN test	8, 32, and 128 g/ml for 24 and 48 hr	No significant genotoxic response was observed
Ahamed et al. [2013]	Fe <sub>3</sub> O <sub>4</sub>	Shape and diameter (TEM) polygonal 24.83 nm; Crystal size (XRD): highest peak at 25.27 nm. Zeta potential (DLS): -23 mV and -26 mV in water and cell culture medium, respectively	Human skin epithelial A431 cells and human lung epithelial A549 cells	Comet assay	25-100 µg/ml for 24 hr	Both A431 and A549 cells exposed to ION exhibited significantly higher DNA damage than controls. A positive linear correlation was observed between intracellular ROS (and DNA damage in A431 cells
Magdolenova et al. [2013]	Uncoated (U-Fe <sub>3</sub> O <sub>4</sub> ), oleate-coated (OC-Fe <sub>3</sub> O <sub>4</sub> ), Fe <sub>3</sub> O <sub>4</sub>	Size (TEM): 5-12 and 5-13 nm, respectively. Primary morphology (TEM): Ellipsoidal particle and octahedral structure, respectively. Surface area (BET): 92 m <sup>2</sup> /g for both. Zeta potential at pH 7: -32 and -2.8 mV, respectively. Magnetic behavior: superparamagnetic and paramagnetic, respectively.	Human lymphoblastoid TK6 cells and PBL	MN test Comet assay	5.4, 27 and 135 µg/ml for 24 hr (TK6) 0.22, 1.13, 5.7, 28.3, and 141 µg/ml (PBL), and 0.57, 2.9, 14.4, 72.0 and 360 µg/ml (TK6), for 2 and 24 hr	U-Fe <sub>3</sub> O <sub>4</sub> were found not to be genotoxic. OC-Fe <sub>3</sub> O <sub>4</sub> induced DNA damage, indicating genotoxic potential
Singh et al. [2013]	Fe <sub>2</sub> O <sub>3</sub> -30 nm; Fe <sub>2</sub> O <sub>3</sub> -bulk	Size (TEM): 29.75 ± 1.87 nm and 2.13 ± 4.15 µm, respectively; Average diameter of Fe <sub>2</sub> O <sub>3</sub> -30 nm(DLS): 363 nm. Zeta potential of Fe <sub>2</sub> O <sub>3</sub> -30 nm (LDV): -18.6 mV. Surface area: 38.02 m <sup>2</sup> /g and 5.76 m <sup>2</sup> /g, respectively	Wistar rat leucocytes Wistar rat PBL and bone marrow cells	Comet assay MN test	Oral treatment. 500, 1,000, 2,000 mg/kg bw for 6, 24, 48, and 72 hr Oral treatment. 500, 1,000, 2,000 mg/kg bw for 48 and 72 hr (PBL) and 24 and 48 hr (bone marrow cells)	All results were not statistically significant at all doses suggesting that these ION were not genotoxic
			Wistar rat bone marrow cells	CA	Oral treatment. 500, 1,000, 2,000 mg/kg bw for 18 and 24 hr	

TABLE I. (continued).

Reference	ION type and surface modification	Physical-chemical characterization	Cellular model/organism	Methods	Treatment conditions	Results
Mesárosová et al. [2014]	Magnetite surface-modified with sodium oleate (SO-Fe <sub>3</sub> O <sub>4</sub> ), SO + polyethylene glycol (SO-PEG-Fe <sub>3</sub> O <sub>4</sub> ), and SO + PEG + poly[lactide-co-glycolic acid] (SO-PEG-PLGA-Fe <sub>3</sub> O <sub>4</sub> )	Magnetite inner core: 7.6 nm. Particle size ( $D_{11}$ ): 44 nm, 76 nm and 155 nm, respectively. Zeta potential: -41.8 mV, -42.3 mV and -50 mV, respectively. Surface area per particle: $6.079 \times 10^{-11}$ cm <sup>2</sup> , $18.137 \times 10^{-11}$ cm <sup>2</sup> and $75.439 \times 10^{-11}$ cm <sup>2</sup> , respectively	Human lung adenocarcinoma A549 cells and human embryonic lung HEL12469 fibroblasts	Comet assay (with and without FPG enzyme)	A549: 0.1–0.5 mM for 24 hr. HEL 12469: 0.05–0.4 mM for 24 hr	A549 cells: all ION regardless the surface coating induced a significant increase in the level of DNA strand breaks. HEL12469: the levels of DNA damage in -treated cells were nearly equal to those observed in control cells. None of the coated ION produced any significant increase in oxidative damage to DNA in either of these cell lines.

5-OH-5MeHyd, 5-hydroxy-5-methylhydantoin; 8-OHdG, 8-hydroxy-2'-deoxyguanosine; APTMS, aminopropyltrimethoxysilane; BET, Brunauer-Emmett-Teller method; BHA, butylated hydroxyanisole; CA, chromosome aberrations; DLS, dynamic light scattering; EDX, energy dispersive X-ray analysis; ELISA, enzyme-linked immunosorbent assay; FapyA, 2,4-diamino-5-formamidopyrimidine; FapyG, 2,6-diamino-4-hydroxy-5-formamidopyrimidine; FPG, formamidopyrimidine-DNA glycosylase; GC, gas chromatography; ION, iron oxide nanoparticles; LDV, laser Doppler velocimetry; LLS, laser light scattering; MN, micronucleus; MS, mass spectrometry; NAC, *N*-acetylcysteine; n/a, not available; PBL, peripheral blood lymphocytes; ROS, reactive oxygen species; SEM, scanning electron microscopy; SSA, specific surface area; TEM, transmission electron microscopy; TEOS, tetraethyl orthosilicate; TG, thymine glycol; VSM, vibrating sample magnetometer; and XRD, X-ray diffraction.

a concentration dependent increase in tail content of DNA compared to control cells, indicating the presence of DNA damage, although no damage to DNA was observed after treatment of the cells with bare or TEOS-coated ION [Hong et al., 2011]. Similarly, primary and oxidative DNA damage (evaluated by means of comet assay) was reported in human lymphoblastoid TK6 cells and primary human leukocytes exposed to oleate-coated nanomagnetite, while no damage was observed in cells treated with uncoated nanomagnetite [Magdolenova et al., 2013]. Employing the same technique, nanohematite was previously found to induce DNA damage in human IMR-90 lung fibroblasts and human BEAS-2B bronchial epithelial cells [Bhattacharya et al., 2009], and also smooth nanomagnetite induced DNA damage in both skin epithelial A431 and lung epithelial A549 cells [Ahamed et al., 2012].

Despite the positive association between ION exposure and genotoxicity noted above, studies showing negative results for ION genotoxicity are more frequent. Karlsson et al. [2008, 2009] exposed A549 cells to ION (Fe<sub>2</sub>O<sub>3</sub> and Fe<sub>3</sub>O<sub>4</sub>) and observed no induction of primary DNA damage as evaluated by the standard comet assay, although Fe<sub>3</sub>O<sub>4</sub> nanoparticles produced increases in oxidative DNA damage. In addition, no increase in MN frequency was found in human lymphoblastoid cells treated with uncoated  $\gamma$ -Fe<sub>2</sub>O<sub>3</sub> nanoparticles or with either uncoated or dextran-coated Fe<sub>3</sub>O<sub>4</sub> nanoparticles [Singh et al., 2012]. Similarly, Fe<sub>2</sub>O<sub>3</sub> (primarily maghemite) and Fe<sub>3</sub>O<sub>4</sub> nanoparticle exposure to Syrian hamster embryo cells Guichard et al. [2012] caused no increase in DNA damage (comet assay) or induction of MN formation. The same tests were applied to assess the genotoxicity associated with exposure of Chinese hamster lung cells to glutamic acid-coated Fe<sub>2</sub>O<sub>3</sub> nanoparticles; although cell redox status was slightly disturbed no significant genotoxic response was observed [Zhang et al., 2012]. Negative results were also obtained in the comet assay with normal human fibroblasts incubated with meso-2,3-dimercaptosuccinic acid (DMSA)-coated maghemite nanoparticles, attributed in part to the DMSA coating that serves as a barrier for a direct contact between nanooxide and fibroblasts, inhibiting potential toxic effects [Auffan et al., 2006]. The mutagenic potential of ION was evaluated by means of the Ames test in two independent studies with negative results as well. First, Weissleder et al. [1989] tested the mutagenicity of AMI-25 ION on five different strains of *S. typhimurium*, with or without metabolic activation, and observed no effects at any concentration evaluated. Later, Bourrinet et al. [2006] found that treatment with ferumoxtran-10, an ultrasmall ION, did not induce any significant increase in the number of revertants, neither in the presence nor in the absence of S9 mix-metabolic activation system.

Short term in vitro genotoxicity tests may be prone to overestimating the in vivo genotoxicity of ION. Although

in vivo genotoxicity studies are time-consuming, expensive and involve ethical issues and complex procedures (e.g. toxicokinetic processes), they have an obvious advantage over in vitro tests. Although there are insufficient in vivo studies in literature on genotoxic effects of ION, the available ones provide important insight into potential in vivo genotoxicity. In particular, Ma et al. [2012] exposed Kunming mice to  $\text{Fe}_3\text{O}_4$  nanoparticles daily for 1 week via intraperitoneal injection in order to determine the potential safe dose range for medical use. Biomarkers of DNA-protein crosslinks and oxidative DNA damage (8-hydroxy-deoxyguanosine) were detected in hepatic and renal tissues, although the latter were more sensitive. Another investigation evaluated genotoxicological effects of a single dose of  $\text{Fe}_2\text{O}_3$  (primarily maghemite) particles orally administered to Wistar rats [Singh et al., 2013]. The results indicated that ION are easily able to pass across the intestinal barrier and although they mainly accumulated in the liver, spleen, kidney, heart and bone marrow, the exposure did not induce genotoxicity in leucocytes (evaluated by the comet assay), chromosomal aberrations in bone marrow cells, or MN in either of these cell types. Contradictory results were also observed among studies evaluating MN frequency in bone marrow cells of mice exposed in vivo to ION. On one hand, positive results were obtained after intraperitoneal exposure to magnetite nanoparticles [Freitas et al., 2002] and intravenous administration of polyaspartic acid-coated magnetite nanoparticles [Sadeghiani et al., 2005]. On the other hand, no increase in MN formation was observed after intraperitoneal injection of ION ( $\text{Fe}_3\text{O}_4$ ) loaded with daunorubicin [Wu et al., 2010] or ION ( $\gamma\text{-Fe}_2\text{O}_3$ ) encapsulated within albumin-based nanospheres [Estevanato et al., 2011], and after intravenous administration of ferumoxtran-10 [Bourrinet et al., 2006]. Nevertheless, a single genotoxicity assay is not sufficient to draw firm conclusions on the genotoxic potential of nanomaterials, since no single test can cover all of the potential forms of DNA damage that might arise [Singh et al., 2009; Zhao and Castranova, 2011]. Thus, negative results obtained in one test do not guarantee that the ION assayed is not genotoxic. Moreover, additional validation of these standard genotoxicity tests when applied to nanoparticles is required before use, in order to be sure that the nanoparticles themselves do not interfere with the test results [Magdolenova et al., 2012].

In view of these studies, it seems that the genotoxic potential of ION is mainly due to their ability to induce DNA breaks and oxidative DNA damage. This ability may be greatly influenced by ION characteristics such as size or surface coating nature. However, given the lack of consistence in the available results, further investigations are required to determine the specific mechanisms underlying DNA damage induced by these nanoparticles.

## Developmental Toxicity

Despite the importance of testing the effects of new commercial materials on embryo and fetal development, the number of studies assessing embryotoxic effects of ION is limited (Table II). The effects of different metal oxide nanoparticles, including  $\text{Fe}_2\text{O}_3$ , on *Xenopus laevis* embryos were recently examined by employing the FETAX (Frog Embryo Teratogenesis Assay Xenopus) approach, a powerful and flexible bioassay for developmental toxicants [Nations et al., 2011]. The results obtained from these analyses showed that  $\text{Fe}_2\text{O}_3$  nanoparticles caused no mortality or significant malformation after 48 hr of exposure; effects noted were limited to snout vent length and total body length at the highest concentration tested (1,000 mg/l). On the basis of their results, the authors proposed that ION have relatively little developmental or teratogenic effects on *X. laevis* during the first 96 hr of embryo life.

Other studies have suggested that ION exposure can lead to developmental effects. Injection of ION ( $\text{Fe}_3\text{O}_4$  coated with dimercaptosuccinic acid) at different doses (40–300 mg/kg) had no adverse effects on weight changes of adult mice even after three months [Noori et al., 2011]. At these doses, ION did not affect gestation and fetal growth, but led to a significant decrease in the offspring growth and maturation after birth, and caused about 70% death before reaching puberty. In the same study a reduction in the number of spermatogonia, spermatocytes, spermatids and mature sperms was observed in male offspring indicating that the presence of ION in the placenta and fetus might disrupt embryo and fetal development. More recently, Zhu et al. [2012a] used early life stages of the zebrafish (*Danio rerio*) to examine the effects of uncoated  $\alpha\text{-Fe}_2\text{O}_3$  on embryonic development. Exposure to doses higher than 10 mg/l initiated developmental toxicity, causing mortality, hatching delay, and malformation in these embryos. Furthermore, in a study employing Syrian hamster embryo cells, ION ( $\text{Fe}_2\text{O}_3$ , primarily maghemite) treatment for 72 hr caused cytotoxicity and intracellular ROS, but not genotoxicity [Guichard et al., 2012].

In another study, potential impacts of ION (ferumoxtran-10) on fertility, reproductive performance, embryotoxicity, fetotoxicity, and teratogenicity were evaluated in rats and rabbits [Bourrinet et al., 2006]. In general, no effects on fertility or early embryonic development were observed either for rats or for rabbits. However, mild maternal toxicity and major fetal skeletal malformations were found in both species.

In summary, because of the adverse effects observed in some studies and our scarce knowledge at the moment of ION developmental toxicity, additional research must be conducted to determine the consequences of ION exposure on embryo and fetal development.

TABLE II. Studies on Developmental Toxicity of ION (Ordered Chronologically)

Reference	ION type and surface modification	Physical-chemical characterization	Cellular model/organism	Methods	Treatment conditions	Results
Bourrinet et al. [2006]	Ferumoxtran-10 (iron oxide core coated with low molecular weight dextran)	Particle diameter (TEM): 30 nm	Sprague-Dawley rats	F0 generation: clinical signs, macroscopic examination of organs (reproductive especially) and pregnancy parameters. F1 generation: external, visceral and skeletal examination, number of live and dead fetuses, fetal weight and sex ratio	Intravenous bolus injection of 2, 6, and 17.9 mg Fe/kg/d during 9 weeks before mating, throughout mating and up to 7th gestation day Intravenous bolus injection of 5, 15 and 50 mg Fe/kg/d throughout 6th up to 18th gestation day	No effects on fertility or early embryonic development. Mildly maternal toxicity and major fetal skeletal malformations were found in rats and rabbits. Therefore, Ferumoxtran-10 was not mutagenic but was teratogenic in rats and rabbits.
Nations et al. [2011]	Fe <sub>2</sub> O <sub>3</sub>	Size (SEM): 17 to 98 nm	Viable embryos of <i>Xenopus laevis</i>	FETAX assay. Evaluated endpoints: mortality, malformations, stage, snout vent length (SVL), and total body length (TBL)	0.001–1,000 mg/l for 96 hr	ION tested did not induce significant mortality for any of the tested concentrations and have relatively little developmental or teratogenic effects on <i>X. laevis</i> during the first 96 hr of embryo life. ION affected SVL and TBL at the highest concentration tested
Noori et al. [2011]	Dimercaptosuccinic acid (DMSA)-coated Fe <sub>3</sub> O <sub>4</sub>	Size (XRD): 3–9 nm FTIR (Fourier Transform MS value (AGFM): 90 μ/g for Fe <sub>3</sub> O <sub>4</sub> , 32 emu/g for DMSA-coated Fe <sub>3</sub> O <sub>4</sub>	Mice of Balb/C strain	Single-dose injected intraperitoneally to the pregnant mice. Detection of ION in the fetal and placental tissues. Histological study of testis	50, 100, 200, and 300 mg/kg on gestation day 8	DMSA-coated Fe <sub>3</sub> O <sub>4</sub> had no adverse effect on weight changes of adult mice even after three months. ION did not affect gestation and fetal growth but led to a significant decrease in the infants' growth and maturation after birth, and caused about 70% death before reaching puberty. A significant reduction on the number of spermatogonia, spermatocytes I, spermatids and mature sperms in seminiferous tubules of male offspring was observed.
Guichard et al. [2012]	Fe <sub>3</sub> O <sub>4</sub> and Fe <sub>2</sub> O <sub>3</sub>	Particle size (TEM, nm): 27 ± 8 (Fe <sub>3</sub> O <sub>4</sub> nano), 156 ± 82 (Fe <sub>3</sub> O <sub>4</sub> micro), 35 ± 14 (Fe <sub>2</sub> O <sub>3</sub> nano), 147 ± 48 (Fe <sub>2</sub> O <sub>3</sub> micro) SSA (BET, m <sup>2</sup> /g): 40 (Fe <sub>3</sub> O <sub>4</sub> nano), 7 (Fe <sub>3</sub> O <sub>4</sub> micro), 39 (Fe <sub>2</sub> O <sub>3</sub> nano), 6 (Fe <sub>2</sub> O <sub>3</sub> micro)	Syrian hamster embryo cells	Acellular ROS by APF staining. Relative cell count (RCC) and EC <sub>50</sub> values. Intracellular ROS by DCFDA staining. Comet assay. Chromosome mutation assays by MN test	0.5–200 μg/cm <sup>2</sup> for 24 and 72 hr	No significant increase in DNA damage was detected from nanosized and microsized Fe <sub>2</sub> O <sub>3</sub> and Fe <sub>3</sub> O <sub>4</sub> . None of the samples tested showed significant induction of MN formation after 24 hr of exposure to both ION. The ROS activity of Fe <sub>3</sub> O <sub>4</sub> and Fe <sub>2</sub> O <sub>3</sub> was detected when particles were incubated in the presence of H <sub>2</sub> O <sub>2</sub> , with a higher intensity for the nanoparticles than for the microparticles. No difference was observed between Fe <sub>3</sub> O <sub>4</sub> nanoparticles and microparticles in ROS generation in acellular condition. ION (Fe <sub>2</sub> O <sub>3</sub> ) treatment for 72 hr caused cytotoxicity and intracellular ROS, but not genotoxicity
Zhu et al. [2012a]	Uncoated α-Fe <sub>2</sub> O <sub>3</sub> (hematite)	Size (TEM): 30 nm	Early life stages of zebrafish ( <i>Danio rerio</i> )	Twenty four wells with 2 ml of ION solution each in triplicate and all the plates were placed in a fish room with controlled light and temperature conditions	100, 50, 10, 5, 1, 0.5, 0.1 mg/l. Time points: 6, 12, 24, 36, 48, 60, 72, 84, 96, 120, 144, and 168 hr	The results showed that doses higher than 10 mg/l of ION instigated developmental toxicity in these embryos, causing a dose-dependent mortality, hatching delay and malformation. Moreover, results suggest that the developmental toxicity of this ION in zebrafish is also time dependent.

AGFM, alternating gradient force magnetometer; APF, 39-(*t*-aminophenyl)fluorescein; BET, Brunauer-Emmett-Teller method; DMSA, dimercaptosuccinate; DCFH-DA, dichloro-dihydro-fluorescein diacetate; FETAX, frog embryo teratogenesis assay *Xenopus*; FTIR, Fourier transform infrared spectroscopy; MN, micronucleus; MS, saturation magnetization; RCC, the relative cell count; ROS, reactive oxygen species; SEM, scanning electron microscope; SLV, snout vent length; SSA, specific surface area; TBL, total body length; TBL, total body length; TEM, transmission electron microscopy; and XRD, X-ray diffraction.

### Neurotoxicity

ION, with diameters in the range of a few tens of nanometers, are able to cross the blood-brain barrier [Wang et al., 2010b]. This ability makes them very suitable for use in a number of medical applications on the nervous system, especially for imaging diagnostics and drug delivery. Indeed, they are envisioned as promising diagnostic and therapeutic tools in neuro-medicine. For example, the conjugation of the drug daunorubicin with ION (oleic acid-capped  $\text{Fe}_3\text{O}_4$ ) nanocomposites for delivery can reduce the neurotoxicity caused by this anticancer drug on rat brains *in vivo*, suggesting a possible application of these nanoparticles to lessen the side effects of cancer therapies [Xu et al., 2012]. For these reasons, the potential neurotoxic effects of ION should be carefully assessed. Table III summarizes the studies on ION neurotoxicity published to date.

As previously described, ROS production is one of the main mechanisms leading to ION-induced toxicity. The brain is particularly vulnerable to ROS damage due to its high content of easily peroxidizable unsaturated fatty acids, high oxygen consumption rate, and relative paucity of antioxidant enzymes compared with other organs [Skaper et al., 1999]. Indeed, oxidative stress is involved in the pathogenesis of neurodegenerative diseases such as Parkinson's, Alzheimer's, and Huntington's [Kim et al., 2012], and oxidative stress is considered a risk factor for ageing [reviewed in Rahman, 2007].

A number of studies have evaluated the effects of different ION on cultured neuronal cells. Pisanic et al. [2007] showed that exposure to increasing concentrations of dimercaptosuccinic acid-coated maghemite nanoparticles caused a dose-dependent reduction of viability and capacity of PC12 cells to extend neurites in response to nerve growth factor. Similarly, treatment of these cells with ION ( $\text{Fe}_3\text{O}_4$ ) at different concentrations also resulted in dose-dependent cytotoxicity [Wu and Sun, 2011]. In this last case, cell cycle arrest in G<sub>2</sub>/M phase and overexpression of the p53 gene without affecting p21 and gadd45, the downstream targets of p53, were also observed after exposure to ION. Moreover, Soenen et al. [2011] tested four different ION types (coated with dextran, carboxydextran, lipid and citrate) on c17.2 neural progenitor cells and observed different cytotoxic potentials; the citrate-coated ION were the most toxic nanoparticles and the lipid-coated ones were the least toxic, under the experimental conditions used. In the same study, a reduction in the length and number of neurites of PC12 cells was also reported for all of the ION tested. More recently, Wu et al. [2013b] concluded that  $\text{Fe}_3\text{O}_4$  nanoparticles decrease neuron viability (PC12 cells), trigger oxidative stress, and activate JNK- and p53-mediated pathways to regulate the cell cycle and apoptosis. However, in contrast with these reports, Kim et al. [2011]

demonstrated that exposure to both PEG-coated ION and nerve growth factor synergistically increased the efficiency of neurite outgrowth in a dose-dependent manner in PC12 cells.

Similar inconsistent effects of ION, resulting primarily from differences in surface coatings, were observed in primary cortical neurons. In a recent study, Rivet et al. [2012] investigated the response of these cells to magnetite nanoparticles coated with aminosilane, dextran, and polydimethylamine, coatings that are frequently used in biomedical applications. They observed different effects depending on nanoparticle dose and coating. Aminosilane-coated ION affected metabolic activity only at high concentrations while leaving the cell membrane intact; dextran-coated ION partially altered viability at high concentrations; and polydimethylamine-coated nanoparticles induced cell death at all of the concentrations tested by swift and complete removal of the plasma membrane. In another study, aminosilane-coated magnetite nanoparticles were found to decrease the viability of primary cortical cultured neurons but in a diverse grade depending on whether ION were positively or negatively charged [Sun et al., 2013].

Glial cells are a group of non-neuronal cells, including astrocytes, microglial cells and oligodendrocytes in the central nervous system, which provide support and protection to neurons. The effects of several ION on astrocytes, the most abundant cells in human brain, and on microglial cells, the resident macrophage-like cells in the central nervous system, have been evaluated in different studies. Au et al. [2007] reported that treatment of immature rat astrocytes with ION ( $\text{Fe}_3\text{O}_4$  or  $\gamma\text{-Fe}_2\text{O}_3$ ) caused inhibition of cell attachment and impeded subsequent growth; the same treatments in mature astrocytes induced mitochondrial uncoupling without altering cell membrane integrity. In addition, incubation of cultured rat astrocytes with citrate- or dimercaptosuccinate-coated ION ( $\gamma\text{-Fe}_2\text{O}_3$ ) caused a time- and concentration-dependent accumulation of cellular iron, but did not lead to any cell toxicity [Geppert et al., 2011, 2012]. The results of these two studies demonstrate that at least some iron can be released from the ION accumulated in astrocytes, and stored as ferritin protein; thus, even the prolonged presence of large amounts of accumulated ION does not harm these cells. In this regard, a recent review on ION uptake and metabolism in brain astrocytes suggests that the efficient uptake of extracellular iron (liberated slowly from ION) by astrocytes, as well as their strong up-regulation of the synthesis of the iron storage protein ferritin, are likely to contribute to their high resistance to iron toxicity. Thus, these cells deal well with an excess of iron and protect the brain against iron-mediated toxicity [Hohnholt and Dringen, 2013]. Apart from these results with rodent cells, to the best of our knowledge only two studies in human astrocytes, with differing results, have been

TABLE III. Studies on Neurotoxicity of ION (Ordered by Cellular Model/Organism Tested)

Reference	ION type and surface modification	Physical-chemical characterization	Cellular model/organism	Methods	Treatment conditions	Results
Pisanic et al. [2007]	DMSA-coated Fe <sub>2</sub> O <sub>3</sub>	Diameter by TEM: 5–12 nm	Rat pheochromocytoma PC12 cells	Live/dead cell staining. Evaluation of neurite number and intercellular contact	0.15, 15, 1.5 mM for 24 hr	Dose-dependent decreases of cell viability and ability to differentiate
Wu and Sun [2011]	Fe <sub>3</sub> O <sub>4</sub>	Size by TEM: 20–50 nm.	Rat pheochromocytoma PC12 cells	MTS assay. Cell cycle analysis. <i>p53</i> , <i>p21</i> and <i>gadd45</i> mRNA expression	25–200 µg/ml for 24h	Dose-dependent decrease of cell viability. Cell cycle arrest in G <sub>2</sub> /M phase. Concentration-dependent increase in <i>p53</i> mRNA levels
Soenen et al. [2011]	Dextran-coated ION (Endorem), carboxydextran-coated ION (Resovist), lipid-coated magnetoliposomes (ML) and citrate-coated very small ION (VSOP)	Size by TEM: 4.8 nm (Endorem), 4.2–4.2 nm (Resovist), 14 nm (ML), 4.0 nm (VSOP). Hydrodynamic diameter: 80–150 nm (Endorem), 62 nm (Resovist), 40 nm (ML), 8.6 nm (VSOP)	Rat pheochromocytoma PC12 cells. Mouse c17.2 neural progenitor cells	ROS detection by NBT. LDH assay. Staining of F-actin and α-tubulin for neurite formation assessment	Endorem (200, 400 µg/ml), Resovist (150, 300 µg/ml), ML (250, 300 µg/ml), and VSOP (200, 600 µg/ml) for 4 and 24 hr	No effect on viability of c17.2 cells. Other cytotoxic effects (ROS production and cell cycle alterations) were obtained c17.2 cells, highly dependent of the type of ION. PC12 cells internalized ION less avidly than c17.2 cells, but still a clear effect of all particles on cell functionality (evaluated as neurite formation) was found
Wu et al. [2013b]	Fe <sub>3</sub> O <sub>4</sub> and <sup>125</sup> I-labeled Fe <sub>3</sub> O <sub>4</sub>	Size by TEM: 30 nm (Fe <sub>3</sub> O <sub>4</sub> ), 36nm ( <sup>125</sup> I-Fe <sub>3</sub> O <sub>4</sub> ). Zeta potential: -9.1 ± 2.2 mV (Fe <sub>3</sub> O <sub>4</sub> ), -8.4 ± 2.1 mV ( <sup>125</sup> I-Fe <sub>3</sub> O <sub>4</sub> )	Rat pheochromocytoma PC12 cells	MTT assay. LDH assay. Annexin V-FITC/PI staining for apoptosis evaluation. Cell cycle analysis. DCFH-DA assay for oxidative stress	25, 50, 100, and 200 µg/ml for 6 and 24 hr	Dose-dependent cytotoxicity and oxidative damage were found after ION treatment. There was an influence on the cell cycle and apoptosis. Cells became arrested at the G <sub>2</sub> /M phase after 24 h of exposure
Kim et al. [2011]	PEG-phospholipid-capped Fe <sub>3</sub> O <sub>4</sub>	Size by TEM: 11 nm	Male Sprague-Dawley rats	Activity of GSH-PX and SOD. Levels of hydrogen peroxide and MDA	Animals intranasally instilled for 1 or 7 d and sacrificed at different days after instillation	After 7 d of instillation, significant changes in all oxidative damage markers were detected in stratum tissue, but just in H <sub>2</sub> O <sub>2</sub> in hippocampal tissue. No significant exposure-related brain histopathological lesions were present
			Rat pheochromocytoma PC12 cells	MTT assay. Measurement of neurite outgrowth	5, 10, 20, and 40 µg/ml for 1, 3, and 5 days	Slight effects on viability at the highest concentration after 3 or 5 d. Morphology and neurite length was also affected. ION promoted neurite outgrowth

TABLE III. (continued).

Reference	ION type and surface modification	Physical-chemical characterization	Cellular model/organism	Methods	Treatment conditions	Results
Rivet et al. [2012]	Amine-, dextran- and PEA-coated Fe <sub>3</sub> O <sub>4</sub>	Core diameter by TEM: ~10 nm. Average hydrodynamic diameter: 45.3 nm (amine-ION), 24.7 nm (dextran-ION), 47.5 nm (PEA-ION)	Cortical neurons isolated from forebrains of 7 day chick embryos	Calcein-AM cell viability assay. MTS assay.	1, 5, and 10% (v/v) of stock particle solution (amine-Fe <sub>3</sub> O <sub>4</sub> : 39.3 mg/ml, PEA-Fe <sub>3</sub> O <sub>4</sub> : 60.5 mg/ml, dextran-Fe <sub>3</sub> O <sub>4</sub> : 53.1 mg/ml) in media for 24 hr	PEA-Fe <sub>3</sub> O <sub>4</sub> induced toxic effects. Amine-Fe <sub>3</sub> O <sub>4</sub> displayed a significant concentration-dependent decrease in metabolic activity but not in viability. Dextran-Fe <sub>3</sub> O <sub>4</sub> partially altered viability at highest concentrations
Sun et al. [2013]	Positively charged AmS-coated ION and negatively charged COOH-AmS-coated ION	Mean hydrodynamic size: ~27 nm. Zeta potential: +23.9 mV (AmS-ION), -17.0 mV (COOH-AmS-ION)	Mouse brain-derived endothelial bEnd.3 cells. Primary neurons and astrocytes isolated from cortices of wild-type mice	MTT assay	0.1–224 µg/ml for 24 hr	Both ION were non-toxic at concentrations below 100 µg/ml in all cell types. At doses higher than 100 µg/ml, bEnd.3 cells showed also no effects, neurons were sensitive to AmS-ION whereas astrocytes were more vulnerable to COOH-AmS-ION
Au et al. [2007]	ION (Fe <sub>3</sub> O <sub>4</sub> or γ-Fe <sub>2</sub> O <sub>3</sub> , exact composition not disclosed)	Information not provided	Cultured brain astrocytes from cortices of newborn Sprague-Dawley rats	LDH assay. MTS assay	10 µg/ml for 6h	Treatment did not alter LDH release but increased MTS activity
Geppert et al. [2011]	DMSA-coated γ-Fe <sub>2</sub> O <sub>3</sub>	Diameter by TEM: 5–20 nm. Average hydrodynamic diameter: 60 nm. Zeta potential: -26 ± 3 mV	Primary cultured brain astrocytes from newborn Wistar rats	Total and ferric iron quantification. LDH assay	500 and 1,000 µM for up to 6 hr	Time- and concentration-dependent accumulation of cellular iron, but no cell toxicity
Geppert et al. [2012]	DMSA-coated γ-Fe <sub>2</sub> O <sub>3</sub>	Diameter by TEM: 5–20 nm. Average hydrodynamic diameter: 60 nm. Zeta potential: -26 ± 3 mV	Primary cultured brain astrocytes from newborn Wistar rats	LDH assay. NRU assay. ROS detection by Rhodamine 123 staining	0.25, 1 and 4 mM for 4 hr	No effects on viability but dose-dependent increases in the iron content and slight increase in oxidative damage
Chen et al. [2012]	DMSA-coated Fe <sub>3</sub> O <sub>4</sub> and DMSA-coated γ-Fe <sub>2</sub> O <sub>3</sub>	Average core diameter by TEM: 9.0 nm (DMSA-Fe <sub>3</sub> O <sub>4</sub> ), 7.8 nm (DMSA-Fe <sub>3</sub> O <sub>4</sub> ). Zeta potential at pH = 7.4: -32.1 ± 3.5 mV (DMSA-Fe <sub>2</sub> O <sub>3</sub> ), -29.2 ± 2.6 mV (DMSA-Fe <sub>3</sub> O <sub>4</sub> )	Human glioma U251 cells	Cell viability assay (mitochondrial activity). LDH assay. Hoechst 33342/PI stain for cell death/apoptosis detection	12.5, 25, 50, and 100 µg/ml for 24 hr. 1.25, 2.5, 5, 10, and 20 µg/ml for 12 hr, then 30 µM H <sub>2</sub> O <sub>2</sub> for 4 hr	DMSA-Fe <sub>2</sub> O <sub>3</sub> had little toxic effect: viability was higher than 85% at all tested concentrations. DMSA-Fe <sub>3</sub> O <sub>4</sub> resulted in a concentration-dependent cytotoxicity. Both ION can enhance H <sub>2</sub> O <sub>2</sub> -induced cell damage dramatically. DMSA-Fe <sub>3</sub> O <sub>4</sub> was more toxic than DMSA-Fe <sub>2</sub> O <sub>3</sub> in the presence of H <sub>2</sub> O <sub>2</sub> . H <sub>2</sub> O <sub>2</sub> -combined DMSA-Fe <sub>3</sub> O <sub>4</sub> treatments directly led cell to death rather than apoptosis
Xiang et al. [2003]	Poly-L-lysine-modified ION	Size by TEM: 20 ± 4.8 nm. Zeta potential at pH = 7: 2.1 ± 1.0 mV; at pH = 9: -9.6 ± 0.91 mV	Human glioma U251 cells	MTT assay	12.5 and 25 µg/ml for 24 hr	ION did not show effect on cell viability

TABLE III. (continued).

Reference	ION type and surface modification	Physical-chemical characterization	Cellular model/organism	Methods	Treatment conditions	Results
Luther et al. [2013]	DMSA-coated ION or BODIPY®-labeled DMSA-coated ION (BP-ION) (predominantly maghemite)	Average hydrodynamic size: $65 \pm 4$ nm (BP-ION), $59 \pm 9$ nm (DMSA-ION). Zeta potential: $49 \pm 2$ mV (BP-ION), $77 \pm 18$ mV (DMSA-ION)	Rat primary microglial cells	LDH assay; GSH assay	150 and 450 $\mu$ M for up to 6 hr	ION caused time- and concentration-dependent increase in the cellular iron content. No effects on viability or oxidative stress were found. However, higher concentrations or longer incubation periods compromised cell viability
Na et al. [2012]	Oligo polyethylene glycol (PEG)-capped Fe <sub>3</sub> O <sub>4</sub>	Diameter by TEM: 11 nm	Murine microglia Bv2 cells	MTT assay	0.0625, 0.125, 0.25, 0.5, 1, and 2 mM for 6 hr	No effects on cell viability
Rosenberg [2012]	Feridex (commercially available superparamagnetic ION)	Information not provided	Murine microglial Bv2 cells	Trypan blue dye exclusion	11.2, 22.4, 56 $\mu$ g Fe for 6h	Dose-dependent increase in intracellular iron concentration with no effect on viability at any concentration tested
Wu et al. [2013a]	Carboxydextran-coated Fe <sub>3</sub> O <sub>4</sub> and carboxydextran-coated Fe <sub>2</sub> O <sub>3</sub>	Average hydrodynamic diameter: 45–60 nm. Zeta potential: $-13.9$ mV (in saline), $-9.01$ mV (in culture medium)	Primary murine microglial cells from forebrains of newborn BALB/c mice	MTT assay. Determination of cytokines (IL-1 $\beta$ and TNF- $\alpha$ )	1, 10, and 50 $\mu$ g Fe/ml for 24 hr	Exposure to ION did not affect cell viability compared to the control group. However, they caused microglial dysfunction by suppressing the production of some cytokines.
Wang et al. [2011]	$\alpha$ -Fe <sub>2</sub> O <sub>3</sub> and $\gamma$ -Fe <sub>2</sub> O <sub>3</sub>	Size by TEM: $22 \pm 5$ nm ( $\alpha$ -Fe <sub>2</sub> O <sub>3</sub> ), $31 \pm 17$ nm ( $\gamma$ -Fe <sub>2</sub> O <sub>3</sub> ). Hydrodynamic diameter in DMEM with 10% FCS: 143 nm ( $\alpha$ -Fe <sub>2</sub> O <sub>3</sub> ), 644 nm ( $\gamma$ -Fe <sub>2</sub> O <sub>3</sub> ). Zeta potential in DMEM with 10% FCS: $-12.5$ mV ( $\alpha$ -Fe <sub>2</sub> O <sub>3</sub> ), $-13$ mV ( $\gamma$ -Fe <sub>2</sub> O <sub>3</sub> ). Specific surface area by BET: 11.2 m <sup>2</sup> /g ( $\alpha$ -Fe <sub>2</sub> O <sub>3</sub> ), 33.2 m <sup>2</sup> /g ( $\gamma$ -Fe <sub>2</sub> O <sub>3</sub> ).	CD-1ICR male mice	Micro-distribution mapping of iron in the brain by SR- $\mu$ XRF. Immunofluorescence microscopy for microglial activation	130 $\mu$ g of ION (6.5 g/l, 10 $\mu$ l per nostril) intranasally instilled every other day for 40 days	Exposure caused microglial proliferation and brain pathological alterations in olfactory bulb, hippocampus and striatum
Hohnholt et al. [2010]	Citrate-coated ION	Diameter by TEM: 5–20 nm, average 10 nm	Murine microglia Bv2 cells	Cell viability assay (mitochondrial ROS measurement (DCFH-DA assay). Nitric oxide assay. Determination of cytokines (IL-1 $\beta$ , IL-6 and TNF- $\alpha$ ).	0.02, 0.2, 2 mol Fe/l for 2–12 hr	Both ION induced cell proliferation, phagocytosis, and release of ROS and NO. Exposure did not cause significant release of inflammatory factors
			Rat oligodendroglial OLN-93 cells	LDH assay. Total and ferric iron quantification	30, 100, and 300 $\mu$ M for 48 hr	Exposure did not cause any detectable loss in cell viability, change in morphology or impaired proliferation, although OLN-93 cells accumulated iron from ION more efficiently than from low molecular weight iron sources

TABLE III. (continued).

Reference	ION type and surface modification	Physical–chemical characterization	Cellular model/organism	Methods	Treatment conditions	Results
Hohnholt et al. [2011]	DMSA-coated ION	Average hydrodynamic diameter: ~60 nm. Zeta potential: $-26 \pm 3$ mV	Rat oligodendroglial OLN-93 cells	LDH assay. MTT assay. ROS detection by Rhodamine 123 staining. GSH and GSSG quantification.	100, 300, and 1,000 $\mu$ M for 24, 48, and 72 hr	Exposure did not cause any acute cytotoxicity or induce oxidative stress
Kenzaoui [2012]	Uncoated Fe <sub>3</sub> O <sub>4</sub> , oleic acid-coated Fe <sub>3</sub> O <sub>4</sub> , PVA-coated ION ( $\gamma$ -Fe <sub>2</sub> O <sub>3</sub> and Fe <sub>3</sub> O <sub>4</sub> )	Hydrodynamic size: $8 \pm 3$ nm (Fe <sub>3</sub> O <sub>4</sub> ), $14\text{--}15$ nm (oleic acid-Fe <sub>3</sub> O <sub>4</sub> ), $25\text{--}30$ nm (PVA-ION). Zeta potential: $-3$ mV (Fe <sub>3</sub> O <sub>4</sub> ), $-30$ mV (oleic acid-Fe <sub>3</sub> O <sub>4</sub> ), $+25$ mV (PVA-ION)	Human brain-derived endothelial cells	MTT assay. Evaluation of free radical formation (DCFH-DA assay). Evaluation of superoxide radicals (dihydroethidium oxidation)	25, 50, 100, 150, and 200 $\mu$ g/ml for 24 hr (MTT assay). 25, 50, 100, and 200 $\mu$ g/ml for 4 hr (DCFH-DA assay and dihydroethidium oxidation)	PVA-ION and uncoated ION were non cytotoxic whereas oleic acid-ION induced decrease of viability at doses higher than 150 $\mu$ g/ml. ROS production was observed for oleic acid-ION and PVA-ION, higher in the last case. No cytotoxicity observed for CNA-ION. Citrate-ION caused a significant decrease in cell viability at concentrations greater than 0.05 mg/ml, and cell viability dropped rapidly at 0.1 mg/ml after 3 hr
Dan et al. [2013]	Cross-linked nanossemblies (CNA)-entrapped Fe <sub>3</sub> O <sub>4</sub> and citrate-coated Fe <sub>3</sub> O <sub>4</sub>	Hydrodynamic size: $90 \pm 10$ nm (citrate-ION), $25 \pm 3$ nm (CNA-ION). Zeta potential at pH=7.4: $-29.5 \pm 3.6$ mV (citrate-ION), $-5.0 \pm 0.6$ mV (can-ION)	Mouse brain-derived endothelial bEnd.3 cells	Resazurin dye assay	Citrate-ION (0.002, 0.02, 0.05, 0.1, and 0.2 mg/ml), CNA-ION (0.2, 0.5, 1, 5, and 10 mg/ml) for 0.5, 3, 6, 12 and 30 hr	No adverse changes in brain of treated rats as compared to controls. However, synaptic transmission and nerve conduction were both affected by exposure: inhibition of all ATPases and acetylcholinesterases
Kumari et al. [2012]	Fe <sub>2</sub> O <sub>3</sub>	Size by TEM: $29.75 \pm 1.87$ nm. Hydrodynamic size: 363 nm. Zeta potential: $-18.6$ mV.	Different tissues of female Wistar rats	Histopathology. Biochemical evaluations of brain total, Na <sup>+</sup> , K <sup>+</sup> , Mg <sup>2+</sup> , and Ca <sup>2+</sup> -ATPases activities, and brain and red blood cells acetylcholinesterases	3, 300 and 1,000 mg/kg/d orally for 28 d	No adverse changes in brain of treated rats as compared to controls. However, synaptic transmission and nerve conduction were both affected by exposure: inhibition of all ATPases and acetylcholinesterases
Bourrinet et al., [2006]	Dextran-covered magnetite (Ferumoxtran-10)	Mean diameter by TEM: 4.2–4.9 nm. Hydrodynamic diameter: 21–30 nm	Male Wistar rats	Observation to detect neurobehavioral, neurovegetative or psychotropic effects during 2 hr after dosing (Irwin test)	2.6, or 13 mg Fe/kg intravenously	Few effects were observed, mainly mydriasis, exophthalmos and effects on spontaneous locomotor activity, that were considered to be nonspecific reactive effects
Wang [2007]	Fe <sub>2</sub> O <sub>3</sub>	Size by TEM: $280 \pm 80$ nm	CD-1CR male mice	Evaluation of iron microdistribution and chemical state in the olfactory bulb and brain stem by SRXRF and XANES. Histopathological observation	Intranasal instillation of 40 mg/kg body weight	Increase of Fe contents was observed in the olfactory nerve and the trigeminus of brain stem. The ratios of Fe (III)/Fe (II) were increased in the olfactory bulb and brain stem. Histopathological observation showed that the neuron fatty degeneration occurred in the CA3 area of hippocampus

TABLE III. (continued).

Reference	ION type and surface modification	Physical-chemical characterization	Cellular model/organism	Methods	Treatment conditions	Results
Kim et al. [2013]	DMSA-Fe <sub>3</sub> O <sub>4</sub> , DMSA-Fe <sub>3</sub> O <sub>4</sub> , PEG-Fe <sub>3</sub> O <sub>4</sub> and PEG-Au-Fe <sub>3</sub> O <sub>4</sub>	Diameter by TEM: 3–15 nm	Adult female Sprague-Dawley rats	Neuropathology assessment and immunodetection with different antibodies	Intraneural injection of ION (10–35 mg/ml, diluted in water to the total of 0.5, 15, or 150 mM of Fe), DMSA (4.4 mg/ml), PEG (4.4 mg/ml)	Biomarkers of inflammation and apoptosis were found to be increased in ION-injected animals. Endothelial and Schwann cells, neurons, and T cells were vulnerable to cell death after DMSA-Fe <sub>3</sub> O <sub>4</sub> exposure
Xu et al. [2012]	Oleic acid-coated Fe <sub>3</sub> O <sub>4</sub> , daunorubicin conjugated oleic acid-coated Fe <sub>3</sub> O <sub>4</sub> nanocomposite	Size by TEM ION: 10–20 nm. Hydrodynamic size nanocomposite: 94.71 nm. Zeta potential nanocomposite: $-21.31 \pm 0.43$ mV	Sprague-Dawley rats	In vivo microdialysis. Measurement of amino acids in cerebrospinal fluid by HPLC	Injection of 15 mg/kg ION or 15 mg/kg nanocomposite	Some alterations in essential amino acids levels were observed after ION injection. For the nanocomposites, the side effect of daunorubicin was visibly cut down, and the time to cause it was apparently shortened as compared with daunorubicin alone.

AmS, aminosilane; DMSA, dimercaptosuccinate; DCFH-DA, dichloro-dihydro-fluorescein diacetate; ESR, electron spin resonance; FITC, fluorescein isothiocyanate; GSH, glutathione (reduced form); GSH-PX, glutathione peroxidase; GSSG, oxidized glutathione; IL, interleukin; LDH, lactate dehydrogenase; MDA, malondialdehyde; MTS, 3-(4,5-dimethylthiazol-2-yl)-5-(3-carboxymethoxyphenyl)-2-(4-sulfophenyl)-2H; MTT, 3-[4, 5-dimethylthiazol-2-yl]-2,5-diphenyltetrazolium bromide; NBT, nitroblue tetrazolium salt; NO, nitric oxide; NRU, neutral red uptake; PEA, poly(dimethylamine)-co-epichlorohydrin-co-ethylendiamine; PEG, polyethylene glycol; PI, propidium iodide; PVA, polyvinylamine; ROS, reactive oxygen species; SOD, superoxide dismutase; SR-μXRF, synchrotron radiation micro-beam X-ray fluorescence; SRXRF, synchrotron radiation X-ray fluorescence; TEM, transmission electron microscopy; TNF, tumor necrosis factor; XANES, X-ray absorption near-edge structure.

published so far. Chen et al. [2012] reported a concentration-dependent cytotoxicity in human glioma (astrocytoma) U251 cells exposed to ION, both  $\text{Fe}_3\text{O}_4$  and  $\gamma\text{-Fe}_2\text{O}_3$ , whereas Xiang et al. [2003] did not observe any effect on viability of the same cells after treatment with poly-L-lysine-modified ION.

Microglia plays a pivotal role in the innate immune responses of the nervous system. Thus, understanding the reactions of microglia cells to nanoparticle exposure is important in the exploration of the neurobiology of nanoparticles. Exposure of cultured rat microglial cells to ION caused a time-, concentration- and temperature-dependent uptake of the particles, predominantly mediated by macropinocytosis and clathrin-mediated endocytosis [Luther et al., 2013], although no cytotoxic effects are usually found after exposure of murine microglial cells to different ION [Na et al., 2012; Rosenberg et al., 2012; Wu et al., 2013a]. In a recent study employing mouse microglial Bv2 cells, treatment with ION ( $\alpha$ - and  $\gamma\text{-Fe}_2\text{O}_3$ ) led to cell proliferation, phagocytosis and generation of ROS and nitric oxide, but did not cause significant release of inflammatory factors, suggesting that microglial activation induced by nanoparticles may act as an alarm and defense system in brain [Wang et al., 2011].

Very few studies have evaluated the potential effects of ION on oligodendrocytes. There are only two studies from Hohnholt's group [Hohnholt et al., 2010, 2011], which reported that viable oligodendroglial OLN-93 cells can efficiently incorporate ION and use iron liberated from accumulated nanoparticles for their own metabolism. Moreover, neither substantial ROS production nor any alteration in the cellular thiol reduction potential was observed after ION exposure.

Exposure of other types of cultured brain cells to ION may induce ROS formation, as found in human brain-derived endothelial cells (used as models of the blood-brain tumor barrier) treated with oleic acid- and polyvinylamine-coated ION ( $\text{Fe}_3\text{O}_4$ ) [Kenzaoui et al., 2012], or have no effects on cell toxicity as reported for cultured mouse brain microvessel endothelial cells exposed to aminosilane-coated magnetite nanoparticles [Sun et al., 2013]. In addition,  $\text{Fe}_3\text{O}_4$  nanoparticles were not cytotoxic to mouse bEnd.3 brain endothelial-derived cells when they were entrapped with cross-linked nanoassemblies, but reduced viability of these cells was observed when the ION were coated with citrate [Dan et al., 2013].

The number of *in vivo* studies on ION neurotoxicity, however, is more restricted. Wistar rats treated daily with  $\text{Fe}_2\text{O}_3$  nanoparticles orally showed that these nanoparticles were distributed in various organs, including brain, 28 days after initiating the treatments. Toxic signs and symptoms, such as dullness, irritation, moribund conditions, but no mortality, were observed in these animals at that time [Kumari et al., 2012]. When the same

animals were exposed intravenously to ferumoxtran-10 nanoparticles, no neurobehavioral, neurovegetative, or psychotropic effects were detected; nevertheless, several physiological responses, including signs of polypnea, exophthalmos and mydriasis, were observed [Bourrinet et al., 2006]. In most of cases, only 50 to 75% of animals were affected and these signs were distributed in a heterogeneous manner over the 2-hr period of observation after dosing. Moreover, after intranasally instilling  $\text{Fe}_3\text{O}_4$  nanoparticles for seven days, Wu et al. [2013a] found a regional distribution of these ION in rat brains that was particularly high in the striatum and hippocampus areas; the exposure induced oxidative damage in the striatum but not in the hippocampus. Similarly, intranasal ION ( $\text{Fe}_2\text{O}_3$ ) exposure in mice caused neuronal fatty degeneration in the hippocampus, led to pathological alterations in olfactory bulb, hippocampus and striatum, as well as causing microglial proliferation, activation and recruitment in these areas, especially in the olfactory bulb [Wang et al., 2007, 2011]. In addition, a significant dose-dependent inhibition of total,  $\text{Na}^+\text{-K}^+$ ,  $\text{Mg}^{2+}$  and  $\text{Ca}^{2+}$ -ATPases in the brain, as well as of brain and red blood cell acetylcholinesterase, were found in exposed animals indicating that synaptic transmission and nerve conduction might have been affected by ION. Recently, Kim et al. [2013] exposed Sprague-Dawley rats to four ION with different surface and core chemistries, namely dimercaptosuccinic acid (DMSA)-coated ION (both  $\gamma\text{-Fe}_2\text{O}_3$  and  $\text{Fe}_3\text{O}_4$ ), PEG-coated  $\text{Fe}_3\text{O}_4$  nanoparticles, and PEG-Au-coated  $\text{Fe}_3\text{O}_4$  nanoparticles. Nerve levels of MAPK/ERK and caspase 3 were analyzed at 48 hr after intraneural injection as indicators of inflammation and apoptosis, respectively, and both were significantly increased in all ION-injected animals. Moreover, macrophages were the main cells to internalize DMSA- $\gamma\text{-Fe}_2\text{O}_3$  nanoparticles in nerve, although no apoptosis was observed in these cells, whereas endothelial and Schwann cells, neurons, and T cells were vulnerable to cell death.

Therefore, the results of all of these studies suggest the possibility of an adverse impact of ION on the nervous system, neuronal cells being the most sensitive ones to their effects, but further investigations are needed to more completely define and characterize this impact.

## CONCLUSIONS

ION are very fascinating nanomaterials that can be used in many current biomedical applications including cell labeling, drug targeting, gene delivery, biosensors, hyperthermia therapy and diagnostics by MRI. These molecules have promising future uses in cancer and other diseases therapy. However, despite the numerous ION applications being explored, insufficient information is available on their potential toxicity.

Medical applications of ION require sufficient intracellular uptake for efficient diagnosis and treatment, leading to a potential risk associated with exposure to these nanoparticles. As these applications are increasing in number and in benefit, it is imperative to comprehensively investigate and elucidate the biological consequences of exposure to ION. In this review the toxicological effects of ION published to date were reviewed, in order to both compile the currently available information on ION toxicity and to elucidate the main gaps of knowledge in this field. The review showed a lack of consensus among the different studies in the literature on ION toxicity, but indicate that the surface coatings and particle size seem to be crucial for ION-induced effects, as they are critical determinants of cellular responses, intensity of effects and potential mechanisms of toxicity. Indeed, it was very difficult to fully compare results across studies mainly because of the different ION employed (surface modification, concentration, size) and the lack of test standardization. Due to the variety of mechanisms leading to nanomaterial induced cell toxicity, a battery of harmonized testing systems would be required to establish the presumptive toxic potential of ION at different levels of biological organization. Moreover, in order to make results comparable across these investigations on ION with different coatings and characteristics, the use of standardized methods is highly desirable.

In conclusion, the significantly increasing use of ION in biomedical applications in parallel with the limited data concerning their effects on human health strongly suggest that additional investigations in this area should be performed, including further studies on the potential long-term effects of exposure to these nanoparticles.

## AUTHOR CONTRIBUTIONS

All authors contributed to the writing and editing of this review, and approved the final manuscript.

## REFERENCES

- Ahamed M, Alhadlaq HA, Alam J, Khan MA, Ali D, Alarafi S. 2013. Iron oxide nanoparticle-induced oxidative stress and genotoxicity in human skin epithelial and lung epithelial cell lines. *Curr Pharm Des* 2013;19:6681–90.
- Alwi R, Telenkov S, Mandelis A, Leshuk T, Gu F, Oladepo S, Michaelian K. 2012. Silica-coated super paramagnetic iron oxide nanoparticles (SPION) as biocompatible contrast agent in biomedical photoacoustics. *Biomed Opt Express* 3:2500–2509.
- Apopa PL, Qian Y, Shao R, Guo NL, Schwegler-Berry D, Pacurari M, Porter D, Shi X, Vallyathan V, Castranova V, et al. 2009. Iron oxide nanoparticles induce human microvascular endothelial cell permeability through reactive oxygen species production and microtubule remodeling. *Part Fibre Toxicol* 6:1.
- Au C, Mutkus L, Dobson A, Riffle J, Lalli J, Aschner M. 2007. Effects of nanoparticles on the adhesion and cell viability on astrocytes. *Biol Trace Elem Res* 120:248–256.
- Au K-W, Liao S-Y, Lee Y-K, Lai W-H, Ng K-M, Chan Y-C, Yip M-C, Ho C-Y, Wu E X, Li RA, et al. 2009. Effects of iron oxide nanoparticles on cardiac differentiation of embryonic stem cells. *Biochem Biophys Res Commun* 379:898–903.
- Auffan M, Decome L, Rose J, Orsiere T, De Meo M, Briois V, Chanéac C, Olivi L, Berge-Lefranc J-L, Botta A, et al. 2006. In vitro interactions between DMSA-coated maghemite nanoparticles and human fibroblasts: A physicochemical and cyto-genotoxic study. *Environ Sci Technol* 40:4367–4373.
- Auffan M, Achouak W, Rose J, Roncato M-A, Chanéac C, Waite D T, Masion A, Woicik J C, Wiesner M R, Bottero J-Y. 2008. Relation between the redox state of iron-based nanoparticles and their cytotoxicity toward *Escherichia coli*. *Environ Sci Technol* 42: 6730–6735.
- Auffan M, Rose J, Bottero J-Y, Lowry GV, Jolivet J-P, Wiesner MR. 2009. Towards a definition of inorganic nanoparticles from an environmental, health and safety perspective. *Nat Nanotechnol* 4: 634–641.
- Berry CC, Wells S, Charles S, Curtis ASG. 2003. Dextran and albumin derivatised iron oxide nanoparticles: Influence on fibroblasts in vitro. *Biomaterials* 24:4551–4557.
- Bhattacharya K, Davoren M, Boertz J, Schins RP, Hoffmann E, Dopp E. 2009. Titanium dioxide nanoparticles induce oxidative stress and DNA-adduct formation but not DNA-breakage in human lung cells. *Part Fibre Toxicol* 6:17.
- Bigini P, Diana V, Barbera S, Fumagalli E, Micotti E, Sitia L, Paladini A, Bisighini C, De Grada L, Coloca L, et al. 2012. Longitudinal tracking of human fetal cells labeled with super paramagnetic iron oxide nanoparticles in the brain of mice with motor neuron disease. *PLoS One* 7:e32326.
- Bjørnerud A, Johansson L. 2004. The utility of superparamagnetic contrast agents in MRI: Theoretical consideration and applications in the cardiovascular system. *NMR Biomed* 17:465–477.
- Borm PJA, Robbins D, Haubold S, Kuhlbusch T, Fissan H, Donaldson K, Schins R, Stone V, Kreyling W, Lademann J, et al. 2006. The potential risks of nanomaterials: A review carried out for ECE-TOC. *Part Fibre Toxicol* 3:11.
- Bourrinet P, Bengele HH, Bonnemain B, Dencausse A, Idee J-M, Jacobs PM, Lewis JM. 2006. Preclinical safety and pharmacokinetic profile of ferumoxtran-10, an ultrasmall superparamagnetic iron oxide magnetic resonance contrast agent. *Invest Radiol* 41:313–324.
- Buyukhatipoglu K, Clyne AM. 2011. Superparamagnetic iron oxide nanoparticles change endothelial cell morphology and mechanics via reactive oxygen species formation. *J Biomed Mater Res A* 96:186–195.
- Buzea C, Pacheco II, Robbie K. 2007. Nanomaterials and nanoparticles: sources and toxicity. *Biointerphases* 2:MR17–MR71.
- Card JW, Zeldin DC, Bonner JC, Nestmann ER. 2008. Pulmonary applications and toxicity of engineered nanoparticles. *Am J Physiol Lung Cell Mol Physiol* 295:1400–1411.
- Carlson C, Hussain SM, Schrand AM, Braydich-Stolle LK, Hess KL, Jones RL, Schlager JJ. 2008. Unique cellular interaction of silver nanoparticles: Size-dependent generation of reactive oxygen species. *J Phys Chem B* 112:13608–13619.
- Chen Z, Yin J-J, Zhou Y-T, Zhang Y, Song L, Song M, Hu S, Gu N. 2012. Dual enzyme-like activities of iron oxide nanoparticles and their implication for diminishing cytotoxicity. *ACS Nano* 6: 4001–4012.
- Dan M, Scott DF, Hardy PA, Wydra RJ, Hilt JZ, Yokel RA, Bae Y. 2013. Block copolymer cross-linked nanoassemblies improve particle stability and biocompatibility of superparamagnetic iron oxide nanoparticles. *Pharm Res* 30:552–561.
- Das M, Saxena N, Dwivedi P D. 2009. Emerging trends of nanoparticles application in food technology: Safety paradigms. *Nanotoxicology* 3:10–18.

- Dwivedi S, Siddiqui MA, Farshori NN, Ahamed M, Musarrat J, Al-Khedhairi AA. 2014. Synthesis, characterization and toxicological evaluation of iron oxide nanoparticles in human lung alveolar epithelial cells. *Colloids Surf B Biointerfaces* 122:209–215.
- Eaton JW, Qian M. 2002. Molecular bases of cellular iron toxicity. *Free Radic Biol Med* 32:833–840.
- Estevanato L, Cintra D, Baldini N, Portilho F, Barbosa L, Martins O, Lacava B, Miranda-Vilela AL, Tedesco AC, Bao S, et al. 2011. Preliminary biocompatibility investigation of magnetic albumin nanosphere designed as a potential versatile drug delivery system. *Int J Nanomed* 6:1709–1717.
- Freitas MLL, Silva LP, Azevedo RB, Garcia VAP, Lacava LM, Grisolia CK, Lucci CM, Morais PC, Da Silva MF, Buske N, et al. 2002. A double-coated magnetite-based magnetic fluid evaluation by cytometry and genetic tests. *J Magn Magn Mater* 252:396–398.
- Geppert M, Hohnholt M, Gaetjen L, Grunwald I, Baumer M, Dringen R. 2009. Accumulation of iron oxide nanoparticles by cultured brain astrocytes. *J Biomed Nanotechnol* 5:285–293.
- Geppert M, Hohnholt MC, Thiel K, Nurnberger S, Grunwald I, Rezwani K, Dringen R. 2011. Uptake of dimercaptosuccinate-coated magnetic iron oxide nanoparticles by cultured brain astrocytes. *Nanotechnology* 22:145101.
- Geppert M, Hohnholt MC, Nurnberger S, Dringen R. 2012. Ferritin up-regulation and transient ROS production in cultured brain astrocytes after loading with iron oxide nanoparticles. *Acta Biomater* 8:3832–3839.
- Gould P. 2006. Nanomagnetism shows in vivo potential. *Nano Today* 1:34–39.
- Guichard Y, Schmit J, Darne C, Gate L, Goutet M, Rousset D, Rasthoix O, Wrobel R, Witschger O, Martin A, et al. 2012. Cytotoxicity and genotoxicity of nanosized and microsized titanium dioxide and iron oxide particles in Syrian hamster embryo cells. *Ann Occup Hyg* 56:631–644.
- Gupta AK, Gupta M. 2005. Synthesis and surface engineering of iron oxide nanoparticles for biomedical applications. *Biomaterials* 26:3995–4021.
- Gurr J-R, Wang ASS, Chen C-H, Jan K-Y. 2005. Ultrafine titanium dioxide particles in the absence of photoactivation can induce oxidative damage to human bronchial epithelial cells. *Toxicology* 213:66–73.
- Hanini A, Schmitt A, Kacem K, Chau F, Ammar S, Gavard J. 2011. Evaluation of iron oxide nanoparticle biocompatibility. *Int J Nanomed* 6:787–794.
- Hiltebrand H, Kuhnel D, Potthoff A, Mackenzie K, Springer A, Schirmer K. 2010. Evaluating the cytotoxicity of palladium/magnetite nano-catalysts intended for wastewater treatment. *Environ Pollut* 158:65–73.
- Hohnholt MC, Dringen R. 2013. Uptake and metabolism of iron and iron oxide nanoparticles in brain astrocytes. *Biochem Soc Trans* 41:1588–1592.
- Hohnholt MC, Geppert M, Dringen R. 2010. Effects of iron chelators, iron salts, and iron oxide nanoparticles on the proliferation and the iron content of oligodendroglial OLN-93 cells. *Neurochem Res* 35:1259–1268.
- Hohnholt MC, Geppert M, Dringen R. 2011. Treatment with iron oxide nanoparticles induces ferritin synthesis but not oxidative stress in oligodendroglial cells. *Acta Biomater* 7:3946–3954.
- Hohnholt MC, Geppert M, Luther EM, Petters C, Bulcke F, Dringen R. 2013. Handling of iron oxide and silver nanoparticles by astrocytes. *Neurochem Res* 38:227–239.
- Hong SC, Lee JH, Lee J, Kim HY, Park JY, Cho J, Lee J, Han D-W. 2011. Subtle cytotoxicity and genotoxicity differences in superparamagnetic iron oxide nanoparticles coated with various functional groups. *Int J Nanomed* 6:3219–3231.
- Huang D-M, Hsiao J-K, Chen Y-C, Chien L-Y, Yao M, Chen Y-K, Ko B-S, Hsu S-C, Tai L-A, Cheng H-Y, et al. 2009. The promotion of human mesenchymal stem cell proliferation by superparamagnetic iron oxide nanoparticles. *Biomaterials* 30:3645–3651.
- Huang S, Li C, Cheng Z, Fan Y, Yang P, Zhang C, Yang K, Lin J. 2012. Magnetic Fe<sub>3</sub>O<sub>4</sub>@mesoporous silica composites for drug delivery and bioadsorption. *J Colloid Interface Sci* 376:312–321.
- Huber DL. 2005. Synthesis, properties, and applications of iron nanoparticles. *Small Weinh Bergstr Ger* 1:482–501.
- Hussain SM, Hess KL, Gearhart JM, Geiss KT, Schlager JJ. 2005. In vitro toxicity of nanoparticles in BRL 3A rat liver cells. *Toxicol Vitro Int J Publ Assoc BIBRA* 19:975–983.
- Iavicoli I, Leso V, Bergamaschi A. 2012. Toxicological effects of titanium dioxide nanoparticles: A review of in vivo studies. *J Nanomater* 2012, Article ID 964381, 36 pages. DOI:10.1155/2012/964381.
- Jeng HA, Swanson J. 2006. Toxicity of metal oxide nanoparticles in mammalian cells. *J Environ Sci Health Part A* 41:2699–2711.
- Johnston H, Pojana G, Zuin S, Jacobsen NR, Moller P, Loft S, Semmler-Behnke M, McGuinness C, Balharry D, Marcomini A, et al. 2013. Engineered nanomaterial risk. Lessons learnt from completed nanotoxicology studies: Potential solutions to current and future challenges. *Crit Rev in Toxicol* 43:1–20.
- Jordan A, Scholz R, Wust P, Fahling H, Roland F. 1999. Magnetic fluid hyperthermia (MFH): Cancer treatment with AC magnetic field induced excitation of biocompatible superparamagnetic nanoparticles. *J Magn Magn Mater* 201:413–419.
- Karlsson HL, Cronholm P, Gustafsson J, Moller L. 2008. Copper oxide nanoparticles are highly toxic: A comparison between metal oxide nanoparticles and carbon nanotubes. *Chem Res Toxicol* 21:1726–1732.
- Karlsson HL, Gustafsson J, Cronholm P, Moller L. 2009. Size-dependent toxicity of metal oxide particles—A comparison between nano- and micrometer size. *Toxicol Lett* 188:112–118.
- Kenzaoui BH, Bernasconi CC, Hofmann H, Juillerat-Jeanneret L. 2012. Evaluation of uptake and transport of ultrasmall superparamagnetic iron oxide nanoparticles by human brain-derived endothelial cells. *Nanomed* 7:39–53.
- Kim JA, Lee N, Kim BH, Rhee WJ, Yoon S, Hyeon T, Park TH. 2011. Enhancement of neurite outgrowth in PC12 cells by iron oxide nanoparticles. *Biomaterials* 32:2871–2877.
- Kim J-E, Shin J-Y, Cho M-H. 2012. Magnetic nanoparticles: An update of application for drug delivery and possible toxic effects. *Arch Toxicol* 86:685–700.
- Kim Y, Kong SD, Chen L-H, Pisanic II TR, Jin S, Shubayev VI. 2013. In vivo nanoneurotoxicity screening using oxidative stress and neuroinflammation paradigms. *Nanomed Nanotechnol Biol Med* 9:1057–1066.
- Konczol M, Ebeling S, Goldenberg E, Treude F, Gminski R, Giere R, Grobety B, Rothen-Rutishauser B, Merfort I, Mersch-Sundermann V. 2011. Cytotoxicity and genotoxicity of size-fractionated iron oxide (magnetite) in A549 human lung epithelial cells: role of ROS, JNK, and NF-kB. *Chem Res Toxicol* 24:1460–1475.
- Kumari M, Rajak S, Singh SP, Kumari SI, Kumar PU, Murty USN, Mahboob M, Grover P, Rahman MF. 2012. Repeated oral dose toxicity of iron oxide nanoparticles: biochemical and histopathological alterations in different tissues of rats. *J Nanosci Nanotechnol* 12:2149–2159.
- Kunzmann A, Andersson B, Vogt C, Feliu N, Ye F, Gabrielsson S, Toprak MS, Buerki-Thurnherr T, Laurent S, Vahter M, et al. 2011. Efficient internalization of silica-coated iron oxide nanoparticles of different sizes by primary human macrophages and dendritic cells. *Toxicol Appl Pharmacol* 253:81–93.

- Landsiedel R, Fabian E, Ma-Hock L, van Ravenzwaay B, Wohlleben W, Wiench K, Oesch F. 2012. Toxicity/biokinetics of nanomaterials. *Arch Toxicol* 86:1021–1060.
- Lee J-H, Huh Y-M, Jun Y, Seo J, Jang J, Song H-T, Kim S, Cho E-J, Yoon H-G, Suh J-S, et al. 2007. Artificially engineered magnetic nanoparticles for ultra-sensitive molecular imaging. *Nat Med* 13: 95–99.
- Levy M, Lagarde F, Maraloiu VA, Blanchin MG, Gendron F, Wilhelm C, Gazeau F. 2010. Degradability of superparamagnetic nanoparticles in a model of intracellular environment: Follow-up of magnetic, structural and chemical properties. *Nanotechnology* 21: 395103.
- Li L, Mak K Y, Shi J, Koon HK, Leung CH, Wong CM, Leung CW, Mak CSK, Chan NMM, Zhong W, et al. 2012. Comparative in vitro cytotoxicity study on uncoated magnetic nanoparticles: effects on cell viability, cell morphology, and cellular uptake. *J Nanosci Nanotechnol* 12:9010–9017.
- Lu C-W, Hung Y, Hsiao J-K, Yao M, Chung T-H, Lin Y-S, Wu S-H, Hsu S-C, Liu H-M, Mou C-Y, et al. 2007. Bifunctional magnetic silica nanoparticles for highly efficient human stem cell labeling. *Nano Lett* 7:149–154.
- Luther EM, Petters C, Bulcke F, Kaltz A, Thiel K, Bickmeyer U, Dringen R. 2013. Endocytotic uptake of iron oxide nanoparticles by cultured brain microglial cells. *Acta Biomater* 9:8454–8465.
- Ma P, Luo Q, Chen J, Gan Y, Du J, Ding S, Xi Z, Yang X. 2012. Intraperitoneal injection of magnetic Fe<sub>3</sub>O<sub>4</sub>-nanoparticle induces hepatic and renal tissue injury via oxidative stress in mice. *Int J Nanomed* 7:4809–4818.
- Magdolenova Z, Lorenzo Y, Collins A, Dusinska M. 2012. Can standard genotoxicity tests be applied to nanoparticles? *J Toxicol Environ Health A* 75:800–806.
- Magdolenova Z, Drlickova M, Henjum K, Rundén-Pran E, Tulinska J, Bilanicova D, Pojana G, Kazimirova A, Barancokova M, Kuricova M, et al. 2013. Coating-dependent induction of cytotoxicity and genotoxicity of iron oxide nanoparticles. *Nanotoxicology* (in press). DOI: 10.3109/17435390.2013.847505.
- Mahmoudi M, Simchi A, Milani A S, Stroeve P. 2009. Cell toxicity of superparamagnetic iron oxide nanoparticles. *J Colloid Interface Sci.* 336:510–518.
- Mahon E, Hristov DL, Dawson KA. 2012. Stabilising fluorescent silica nanoparticles against dissolution effects for biological studies. *Chem Commun* 48:7970–7972.
- Malvindi MA, De Matteis V, Galeone A, Brunetti V, Anyfantis GC, Athanassiou A, Cingolani R, Pompa PP. 2014. Toxicity assessment of silica coated iron oxide nanoparticles and biocompatibility improvement by surface engineering. *PLoS One* 9:e85835.
- McBain SC, Griesenbach U, Xenariou S, Keramane A, Batich CD, Alton EFWF, Dobson J. 2008. Magnetic nanoparticles as gene delivery agents: Enhanced transfection in the presence of oscillating magnet arrays. *Nanotechnology* 19:405102.
- Mesárošová M, Kozics K, Bábelová A, Regendová E, Pastorek M, Vnučková D, Bulíková B, Rázga F, Gábelová A. 2014. The role of reactive oxygen species in the genotoxicity of surface-modified magnetite nanoparticles. *Toxicol Lett* 226:303–313.
- Møller P, Jacobsen NR, Folkmann JK, Danielsen PH, Mikkelsen L, Hemmingsen JG, Vesterdal LK, Forchhammer L, Wallin H, Loft S. 2010. Role of oxidative damage in toxicity of particulates. *Free Radic Res* 44:1–46.
- Na HB, Palui G, Rosenberg JT, Ji X, Grant SC, Mattoussi H. 2012. Multidentate catechol-based polyethylene glycol oligomers provide enhanced stability and biocompatibility to iron oxide nanoparticles. *ACS Nano* 6:389–399.
- Naqvi S, Samim M, Abidin M, Ahmed FJ, Maitra A, Prashant C, Dinda AK. 2010. Concentration-dependent toxicity of iron oxide nanoparticles mediated by increased oxidative stress. *Int J Nanomed* 5:983–989.
- Nations S, Wages M, Cañas JE, Maul J, Theodorakis C, Cobb GP. 2011. Acute effects of Fe<sub>2</sub>O<sub>3</sub>, TiO<sub>2</sub>, ZnO and CuO nanomaterials on *Xenopus laevis*. *Chemosphere* 83:1053–1061.
- Nel A, Xia T, Mädler L, Li N. 2006. Toxic potential of materials at the nanolevel. *Science* 311:622–627.
- Noori A, Parivar K, Modaresi M, Messripour M, Yousefi MH, Amiri GR. 2011. Effect of magnetic iron oxide nanoparticles on pregnancy and testicular development of mice. *Afr J Biotechnol* 10: 1221–1227.
- Oberdorster G, Stone V, Donaldson K. 2008. Toxicology of nanoparticles: A historical perspective. *Nanotoxicology* 1:2–25.
- Pan Y, Leifert A, Ruau D, Neuss S, Bornemann J, Schmid G, Brandau W, Simon U, Jahnke-Dechent W. 2009. Gold nanoparticles of diameter 1.4 nm trigger necrosis by oxidative stress and mitochondrial damage. *Small Weinh Bergstr Ger* 5:2067–2076.
- Pankhurst QA, Connolly J, Jones SK, Dobson J. 2003. Applications of magnetic nanoparticles in biomedicine. *J Phys Appl Phys* 36: r167.
- Pisanic TR 2nd, Blackwell JD, Shubayev VI, Fiñones RR, Jin S. 2007. Nanotoxicity of iron oxide nanoparticle internalization in growing neurons. *Biomaterials* 28:2572–2581.
- Rahman K. 2007. Studies on free radicals, antioxidants, and co-factors. *Clin Interv Aging* 2:219–236.
- Rivet CJ, Yuan Y, Borca-Tasciuc D-A, Gilbert RJ. 2012. Altering iron oxide nanoparticle surface properties induce cortical neuron cytotoxicity. *Chem Res Toxicol* 25:153–161.
- Rosenberg JT, Sachi-Kocher A, Davidson MW, Grant SC. 2012. Intracellular SPIO labeling of microglia: High field considerations and limitations for MR microscopy. *Contrast Media Mol Imaging* 7: 121–129.
- Rosi NL, Mirkin CA. 2005. Nanostructures in biodiagnostics. *Chem Rev* 105:1547–1562.
- Sadeghiani N, Barbosa LS, Silva LP, Azevedo RB, Morais PC, Lacava ZGM. 2005. Genotoxicity and inflammatory investigation in mice treated with magnetite nanoparticles surface coated with polyaspartic acid. *J Magn Magn Mater* 289:466–468.
- Salata O. 2004. Applications of nanoparticles in biology and medicine. *J Nanobiotechnol* 2:3.
- Santhosh PB, Ulrih NP. 2013. Multifunctional superparamagnetic iron oxide nanoparticles: Promising tools in cancer theranostics. *Cancer Lett* 336:8–17.
- Schäfer R, Kehlbach R, Wiskirchen J, Bantleon R, Pintaske J, Brehm BR, Gerber A, Wolburg H, Claussen CD, Northoff H. 2007. Transferrin receptor upregulation: In vitro labeling of rat mesenchymal stem cells with superparamagnetic iron oxide. *Radiology* 244:514–523.
- Shander A, Cappellini MD, Goodnough LT. 2009. Iron overload and toxicity: The hidden risk of multiple blood transfusions. *Vox Sang* 97:185–197.
- Shubayev VI, Pisanic TR 2nd, Jin S. 2009. Magnetic nanoparticles for theranostics. *Adv Drug Deliv Rev* 61:467–477.
- Singh N, Manshian B, Jenkins GJS, Griffiths SM, Williams PM, Maffei TGG, Wright CJ, Doak SH. 2009. Nanogenotoxicology: The DNA damaging potential of engineered nanomaterials. *Biomaterials* 30:3891–3914.
- Singh N, Jenkins GJS, Asadi R, Doak SH. 2010. Potential toxicity of superparamagnetic iron oxide nanoparticles (SPIO). *Nano Reviews* 2010, 1:5358. DOI: 10.3402/nano.v1i0.5358.
- Singh N, Jenkins GJS, Nelson BC, Marquis BJ, Maffei TGG, Brown AP, Williams PM, Wright CJ, Doak SH. 2012. The role of iron redox state in the genotoxicity of ultrafine superparamagnetic iron oxide nanoparticles. *Biomaterials* 33:163–170.

- Singh SP, Rahman MF, Murty USN, Mahboob M, Grover P. 2013. Comparative study of genotoxicity and tissue distribution of nano and micron sized iron oxide in rats after acute oral treatment. *Toxicol Appl Pharmacol* 266:56–66.
- Skaper SD, Floreani M, Cecon M, Facci L, Giusti P. 1999. Excitotoxicity, oxidative stress, and the neuroprotective potential of melatonin. *Ann NY Acad Sci* 890:107–118.
- Soenen SJH, De Cuyper M. 2009. Assessing cytotoxicity of (iron oxide-based) nanoparticles: An overview of different methods exemplified with cationic magnetoliposomes. *Contrast Media Mol Imaging* 4:207–219.
- Soenen SJH, De Cuyper M. 2010. Assessing iron oxide nanoparticle toxicity in vitro: Current status and future prospects. *Nanomedicine* 5:1261–1275.
- Soenen SJH, Himmelreich U, Nuytten N, De Cuyper M. 2011. Cytotoxic effects of iron oxide nanoparticles and implications for safety in cell labeling. *Biomaterials* 32:195–205.
- Stohs SJ, Bagchi D. 1995. Oxidative mechanisms in the toxicity of metal ions. *Free Radic Biol Med* 18:321–336.
- Stroh A, Zimmer C, Gutzeit C, Jakstadt M, Marschke F, Jung T, Pilgrimm H, Grune T. 2004. Iron oxide particles for molecular magnetic resonance imaging cause transient oxidative stress in rat macrophages. *Free Radic Biol Med* 36:976–984.
- Suh WH, Suslick KS, Stucky GD, Suh Y-H. 2009. Nanotechnology, nanotoxicology, and neuroscience. *Prog Neurobiol* 87:133–170.
- Sun C, Lee JSH, Zhang M. 2008. Magnetic nanoparticles in MR imaging and drug delivery. *Adv Drug Deliv Rev* 60:1252–1265.
- Sun Z, Yathindranath V, Worden M, Thliveris JA, Chu S, Parkinson FE, Hegmann T, Miller DW. 2013. Characterization of cellular uptake and toxicity of aminosilane-coated iron oxide nanoparticles with different charges in central nervous system-relevant cell culture models. *Int J Nanomed* 8:961–970.
- Szalay B, Tátrai E, Nyíró G, Vezér T, Dura G. 2012. Potential toxic effects of iron oxide nanoparticles in vivo and in vitro experiments. *J Appl Toxicol* 32:446–453.
- Taton TA. 2002. Nanostructures as tailored biological probes. *Trends Biotechnol* 20:277–279.
- Tong L, Zhao M, Zhu S, Chen J. 2011. Synthesis and application of superparamagnetic iron oxide nanoparticles in targeted therapy and imaging of cancer. *Front Med* 5:379–387.
- Unfried K, Albrecht C, Klotz L-O, Von Mikecz A, Grether-Beck S, Schins RPF. 2007. Cellular responses to nanoparticles: Target structures and mechanisms. *Nanotoxicology* 1:52–71.
- Wang B, Feng WY, Wang M, Shi JW, Zhang F, Ouyang H, Zhao YL, Chai ZF, Huang YY, Xie YN, et al. 2007. Transport of intranasally instilled fine Fe<sub>2</sub>O<sub>3</sub> particles into the brain: Microdistribution, chemical states, and histopathological observation. *Biol Trace Elem Res* 118:233–243.
- Wang D, Wang L-H, Zhao Y, Lu Y-P, Zhu L. 2010a. Hypoxia regulates the ferrous iron uptake and reactive oxygen species level via divalent metal transporter 1 (DMT1) Exon1B by hypoxia-inducible factor-1. *IUBMB Life* 62:629–636.
- Wang J, Chen Y, Chen B, Ding J, Xia G, Gao C, Cheng J, Jin N, Zhou Y, Li X, et al. 2010b. Pharmacokinetic parameters and tissue distribution of magnetic Fe<sub>3</sub>O<sub>4</sub> nanoparticles in mice. *Int J Nanomed* 5:861–866.
- Wang Y, Wang B, Zhu M-T, Li M, Wang H-J, Wang M, Ouyang H, Chai Z-F, Feng W-Y, Zhao Y-L. 2011. Microglial activation, recruitment and phagocytosis as linked phenomena in ferric iron nanoparticle exposure. *Toxicol Lett* 205:26–37.
- Wang YX, Hussain SM, Krestin GP. 2001. Superparamagnetic iron oxide contrast agents: Physicochemical characteristics and applications in MR imaging. *Eur Radiol* 11:2319–2331.
- Weissleder R, Stark DD, Engelstad BL, Bacon BR, Compton CC, White DL, Jacobs P, Lewis J. 1989. Superparamagnetic iron oxide: pharmacokinetics and toxicity. *Am J Roentgenol* 152:167–173.
- Wu H-Y, Chung M-C, Wang C-C, Huang C-H, Liang H-J, Jan T-R. 2013a. Iron oxide nanoparticles suppress the production of IL-1beta via the secretory lysosomal pathway in murine microglial cells. *Part Fibre Toxicol* 10:46.
- Wu H-Y, Chung M-C, Wang C-C, Huang C-H, Liang H-J, Jan T-R. 2013b. Iron oxide nanoparticles suppress the production of IL-1beta via the secretory lysosomal pathway in murine microglial cells. *Part Fibre Toxicol* 10:46.
- Wu J, Sun J. 2011. Investigation on mechanism of growth arrest induced by iron oxide nanoparticles in PC12 cells. *J Nanosci Nanotechnol* 11:11079–11083.
- Wu J, Ding T, Sun J. 2013c. Neurotoxic potential of iron oxide nanoparticles in the rat brain striatum and hippocampus. *Neurotoxicology* 34:243–253.
- Wu W, Chen B, Cheng J, Wang J, Xu W, Liu L, Xia G, Wei H, Wang X, Yang M, et al. 2010. Biocompatibility of Fe<sub>3</sub>O<sub>4</sub>/DNR magnetic nanoparticles in the treatment of hematologic malignancies. *Int J Nanomed* 5:1079–1084.
- Xia T, Kovichich M, Liang M, Meng H, Kabehie S, George S, Zink JJ, Nel AE. 2009. Polyethyleneimine coating enhances the cellular uptake of mesoporous silica nanoparticles and allows safe delivery of siRNA and DNA constructs. *ACS Nano* 3:3273–3286.
- Xiang J-J, Tang J-Q, Zhu S-G, Nie X-M, Lu H-B, Shen S-R, Li X-L, Tang K, Zhou M, Li G-Y. 2003. IONP-PLL: a novel non-viral vector for efficient gene delivery. *J Gene Med* 5:803–817.
- Xu P, Li J, Chen B, Wang X, Cai X, Jiang H, Wang C, Zhang H. 2012. The real-time neurotoxicity analysis of Fe<sub>3</sub>O<sub>4</sub> nanoparticles combined with daunorubicin for rat brain in vivo. *J Biomed Nanotechnol* 8:417–423.
- Yang C-Y, Hsiao J-K, Tai M-F, Chen S-T, Cheng H-Y, Wang J-L, Liu H-M. 2011. Direct labeling of hMSC with SPIO: the long-term influence on toxicity, chondrogenic differentiation capacity, and intracellular distribution. *Mol Imaging Biol* 13:443–451.
- Ying E, Hwang H-M. 2010. In vitro evaluation of the cytotoxicity of iron oxide nanoparticles with different coatings and different sizes in A3 human T lymphocytes. *Sci Total Environ* 408:4475–4481.
- Yu M, Huang S, Yu KJ, Clyne AM. 2012. Dextran and polymer polyethylene glycol (PEG) coating reduce both 5 and 30 nm iron oxide nanoparticle cytotoxicity in 2D and 3D cell culture. *Int J Mol Sci* 13:5554–5570.
- Zhang T, Qian L, Tang M, Xue Y, Kong L, Zhang S, Pu Y. 2012. Evaluation on cytotoxicity and genotoxicity of the L-glutamic acid coated iron oxide nanoparticles. *J Nanosci Nanotechnol* 12:2866–2873.
- Zhao J, Castranova V. 2011. Toxicology of nanomaterials used in nanomedicine. *J Toxicol Environ Health B Crit Rev* 14:593–632.
- Zhu M-T, Wang Y, Feng W-Y, Wang B, Wang M, Ouyang H, Chai Z-F. 2010. Oxidative stress and apoptosis induced by iron oxide nanoparticles in cultured human umbilical endothelial cells. *J Nanosci Nanotechnol* 10:8584–8590.
- Zhu M-T, Wang B, Wang Y, Yuan L, Wang H-J, Wang M, Ouyang H, Chai Z-F, Feng W-Y, Zhao Y-L. 2011. Endothelial dysfunction and inflammation induced by iron oxide nanoparticle exposure: Risk factors for early atherosclerosis. *Toxicol Lett* 203:162–171.
- Zhu X, Tian S, Cai Z. 2012a. Toxicity assessment of iron oxide nanoparticles in zebrafish (*Danio rerio*) early life stages. *PLoS One* 7: e46286.
- Zhu X-M, Wang Y-XJ, Leung KC-F, Lee S-F, Zhao F, Wang D-W, Lai JMY, Wan C, Cheng CHK, Ahuja AT. 2012b. Enhanced cellular uptake of aminosilane-coated superparamagnetic iron oxide nanoparticles in mammalian cell lines. *Int J Nanomed* 7:953–964.